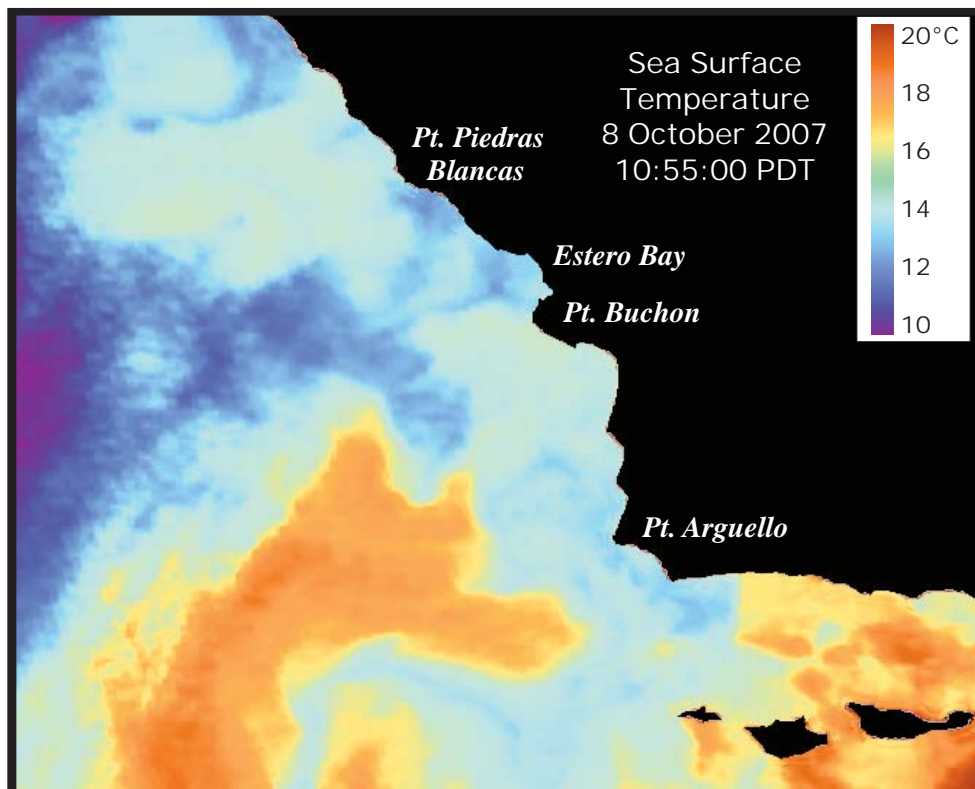


**City of Morro Bay and
Cayucos Sanitary District**

OFFSHORE MONITORING AND REPORTING PROGRAM

QUARTERLY REPORT

WATER-COLUMN SAMPLING OCTOBER 2007 SURVEY



Marine Research Specialists

**3140 Telegraph Rd., Suite A
Ventura, California 93003**

Report to

**City of Morro Bay and
Cayucos Sanitary District**

**955 Shasta Avenue
Morro Bay, California 93442
(805) 772-6272**

**OFFSHORE MONITORING
AND
REPORTING PROGRAM**

QUARTERLY REPORT

**WATER-COLUMN SAMPLING
OCTOBER 2007**

Prepared by

**Douglas A. Coats
Tyler Eck
Bonnie Luke**

Marine Research Specialists

**3140 Telegraph Rd., Suite A
Ventura, California 93003**

**Telephone: (805) 644-1180
Telefax: (805) 289-3935
E-mail: Doug.Coats@mrsenv.com**

November 2007

marine research specialists

3140 Telegraph Road, Suite A · Ventura, CA 93003 · (805) 644-1180

Mr. Bruce Keogh
Wastewater Division Manager
City of Morro Bay
955 Shasta Avenue
Morro Bay, CA 93442

28 November 2007

Reference: Quarterly Receiving-Water Report – October 2007

Dear Mr. Keogh:

Enclosed is the Quarterly Report for the Water-Quality Survey conducted on Tuesday, 9 October 2007. This fourth-quarter survey assessed the effectiveness of effluent dispersion during fall oceanographic conditions. Based on quantitative analyses of continuous instrumental measurements and qualitative visual observations, the wastewater discharge was found to be in compliance with the receiving-water limitations specified in the NPDES discharge permit, and with the objectives of the California Ocean Plan.

High-precision measurements clearly delineated discharge-related perturbations in five of the six seawater properties at four of the sixteen sampling stations. Two of the perturbations were measured within a few meters of the discharge and demonstrated that the diffuser structure was achieving dilution levels that significantly exceeded those anticipated by modeling and outfall design criteria. All of the measurements were indicative of low organic loading within the discharged wastewater, and of an outfall operating as designed.

Please contact the undersigned if you have any questions regarding the attached report.

Sincerely,

Douglas A. Coats, Ph.D.
Program Manager

Enclosure (Five Report Copies)

I certify under penalty of law that this document and all attachments were prepared under my direction or supervision in accordance with a system designed to assure that qualified personnel properly gather and evaluate the information submitted. Based on my inquiry of the person or persons who manage the system, or those persons directly responsible for gathering the information, the information submitted is, to the best of my knowledge and belief, true, accurate, and complete. I am aware that there are significant penalties for submitting false information, including the possibility of fine and imprisonment for knowing violations.

Mr. Bruce Ambo
City of Morro Bay

Date _____

TABLE OF CONTENTS

LIST OF FIGURES	i
LIST OF TABLES	ii
INTRODUCTION	1
STATION LOCATIONS	2
METHODS	11
<i>Auxiliary Measurements</i>	12
<i>Instrumental Measurements</i>	12
<i>Temporal Trends in the DO and pH Sensors</i>	14
RESULTS.....	15
<i>Beneficial Use</i>	15
<i>Ambient Seawater Properties</i>	16
<i>Lateral Variability</i>	18
<i>Discharge-Related Perturbations</i>	21
<i>Initial Dilution Computations</i>	24
DISCUSSION	26
<i>Outfall Performance</i>	26
<i>NPDES Permit Limits</i>	26
<i>Light Transmittance</i>	27
<i>Dissolved Oxygen</i>	27
<i>pH</i>	28
<i>Temperature and Salinity</i>	28
<i>Conclusions</i>	28
REFERENCES	29

APPENDICES

- A. Water-Quality Profiles and Cross Sections
- B. Tables of Profile Data and Standard Observations

LIST OF FIGURES

Figure 1. Regional Setting of Receiving-Water Sampling Stations within Estero Bay	3
Figure 2. Offshore Water Sampling Locations on 9 October 2007.....	5
Figure 3. Drifter Trajectory on 9 October 2007	9
Figure 4. Estero Bay Tidal Level during the Field Survey of 9 October 2007	10
Figure 5. 30-Day Running Mean Upwelling Index (m ³ /s/100m of coastline) Offshore Estero Bay.....	10

LIST OF TABLES

Table 1. Description of Receiving-Water Monitoring Stations 4
Table 2. Average Coordinates of Vertical Profiles during the July 2007 Survey 8
Table 3. Instrumental Specifications for CTD Profiler..... 13
Table 4. Discharge-Related Water-Property Anomalies 22

INTRODUCTION

The City of Morro Bay and the Cayucos Sanitary District (MBCSD) jointly own the wastewater treatment plant operated by the City of Morro Bay. A National Pollutant Discharge Elimination System (NPDES) permit, modifying secondary treatment requirements, was originally issued to the MBCSD in March 1985. The permit was issued by Region IX of the U.S. Environmental Protection Agency (USEPA) and the Central Coast California Regional Water Quality Control Board (RWQCB). Following extensive evaluation processes, the permit has been re-issued twice, once in March of 1993 (RWQCB-USEPA 1993ab) and again in December 1998 (RWQCB-USEPA 1998ab).

As part of the current permit provisions, the previous monitoring program was modified to better evaluate short and long-term effects of the discharge on receiving waters, benthic sediments, and infaunal communities (RWQCB-EPA 1998b). The program continued to include a requirement for receiving-water-quality monitoring performed on a seasonal basis. The four quarterly surveys are intended to record ambient water properties that approximate winter, spring, summer, and fall conditions. In keeping with seasonal synopses, this quarterly report summarizes the results of water-quality sampling conducted on 9 October 2007. Specifically, this fourth-quarter survey captures ambient oceanographic conditions along the central California coast during the early fall season.

The water-quality surveys also provide timely assessments of the performance of the diffuser structure in dispersing wastewater within stratified receiving waters. Any significant, recent damage to the diffuser structure would be revealed by a decline in the level of wastewater dispersion measured in this survey compared to that of prior surveys, and compared to design specifications. As described in this report, no such decline was observed in the October 2007 field survey.

Both monitoring objectives were achieved through an evaluation of the water-column profiles and cross sections of water-property distributions that are presented in Appendix A. Appendix B tabulates instrumental measurements and standard field observations. These data were used to assess compliance with the objectives of the California Ocean Plan (COP) as promulgated by the NPDES discharge permit.

The October 2007 field survey was the thirty-sixth receiving-water survey to be conducted under the monitoring provisions of the current permit. Compared to the previous permit, the number of stations increased from 11 to 16, and the stations were relocated closer (≤ 100 m) to the diffuser structure. Sampling at these more closely spaced stations could only be achieved because of the availability of increased navigational accuracy that resulted from implementation of the differential global positioning satellite (DGPS) system. This system was commissioned during the March 1998 survey (MRS 1998a) and was subsequently employed in the precise determination of the open section of the diffuser structure during a diver survey on 29 September 1998 (MRS 1998bc).

The current sampling design also allowed surveying to be conducted more rapidly than previous surveys by eliminating the requirement for collection of discrete water samples at individual stations. These samples were collected using Niskin bottles, which was time consuming and interrupted the continuity of instrumental measurements collected by the CTD¹ instrument package. Continuous deployment of the CTD between stations now provides a more synoptic snapshot of the water properties immediately

¹ Conductivity, Temperature, and Depth (CTD) were the original measurements recorded by this standard oceanographic instrument package, but the moniker now connotes an electronic instrument package with a broader suite of probes and sensors capable of *in situ* measurement of dissolved oxygen, transmissivity, and pH.

surrounding the diffuser structure. Consequently, the extent of the effluent plume and the amplitude of its associated water-property anomalies can be more precisely determined. The sensitive sensors onboard the CTD instrument package are capable of detecting minute changes in water properties. These sensors are described in the Methods Section below.

Surveys conducted prior to 1999 rarely detected the effluent plume because sampling stations were too widely separated to resolve a dilute wastewater signature that is highly localized around the outfall diffuser. With the implementation of the current sampling design in 1999, the presence of well-mixed effluent near the diffuser structure was found in all 36 of the subsequent water-quality surveys (MRS 2000, 2001, 2002, 2003, 2004, 2005, 2006, 2007), including the one described in this report. Moreover, improved navigation in concert with the denser sampling pattern more precisely delineated the lateral extent of the discharge-related perturbations in seawater properties.

Precision navigation is important for assessing compliance because most receiving-water limitations apply only beyond the narrow zone of initial dilution (ZID) that surrounds the outfall. Additionally, the amplitudes of the effluent-related perturbations can be better determined by the denser sampling pattern. The amplitudes of discharge-related salinity anomalies reveal the details of dilution as the effluent plume disperses within receiving waters. Measured dilution factors lend insight into the current operational performance of the outfall and diffuser structure. As described in this report, the presence of dilute effluent undergoing turbulent mixing within the weakly stratified water column north of the diffuser structure was delineated by the data collected during the October 2007 survey.

STATION LOCATIONS

The water-sampling stations surround the area where effluent is discharged within Estero Bay (Figure 1). The 1,450 m long outfall pipe, which carries the effluent from the onshore treatment plant, terminates at the diffuser structure, which lies on the seafloor approximately 827 m from the shoreline.² The diffuser structure itself extends an additional 52 m toward the northwest from the outfall terminus.

Twenty-eight of the 34 available ports discharge effluent along a 42 m section of the diffuser structure. The other six diffuser ports remain closed to improve dispersion by increasing the ejection velocity from the open ports. For a given flow rate, the diffuser ports were hydraulically designed to create a turbulent ejection jet, which serves to rapidly mix effluent with receiving seawater immediately upon discharge. Additional turbulent mixing occurs as the buoyant plume of dilute effluent rises through the water column. Most of this buoyancy-induced mixing occurs within a zone of initial dilution (ZID), whose lateral extent in modeling studies is considered to be approximately 15 m from the centerline of the diffuser structure. Beyond the ZID, the energetic waves, tides, and coastal currents within Estero Bay further disperse the discharge plume within the open-ocean receiving waters. Areas of special concern, such as sanctuaries and estuaries, are too distant to be affected by the effluent discharge. For example, the southern boundary of the Monterey Bay National Marine Sanctuary is located 38 km to the north, near Cambria Rock.

² This distance was determined from a navigational survey conducted on 6 July 2005 to benchmark the locations of the current surfzone sampling stations along the shoreline adjacent to the diffuser structure. The beginning of the section of the diffuser structure containing open diffuser ports lies directly offshore surfzone Station C (Figure 1). This closest-approach shoreline position was determined at the water's edge when the tidal level was +2.7 ft, referenced to mean lower low water (MLLW).



Figure 1. Regional Setting of Receiving-Water Sampling Stations within Estero Bay

Similarly, the entrance to the Morro Bay National Estuary lies 2.8 km south of the discharge and direct seawater exchange between the discharge point and the Bay is restricted by the southerly orientation of the mouth of the Bay, and by the presence of Morro Rock. Morro Rock is the largest physiographic feature of the adjacent coastline and extends into Estero Bay approximately 2 km south of the point of discharge (Figure 1). Its presence further restricts the direct exchange of seawater between the discharge point and the Bay.

Near the diffuser, prevailing currents generally follow bathymetric contours, which parallel the north-south trend of the adjacent coastline. Because of the rapid initial mixing achieved within 15 m of the diffuser structure, impingement of unmixed effluent onto the adjacent coastline 827 m away is highly unlikely. Nevertheless, water samples are regularly collected along the shoreline at the surfzone sampling stations shown in Figure 1. These surfzone samples are analyzed for total and fecal coliform levels. Results of these analyses are reported in monthly operational summaries and in annual reports. The instances of elevated beach coliform levels that are occasionally observed have resulted from onshore non-point sources rather than the discharge of disinfected wastewater from the MBCSD outfall (MRS 2000, 2001, 2002, 2003, 2004, 2005, 2006, 2007).

As shown in Figure 2, the water-sampling design consists of 16 fixed offshore stations located within 100 m of the outfall diffuser structure. The target locations of the 16 offshore sampling stations are indicated by the red ⊙ symbols in the Figure. The stations are situated at three distances relative to the center of the diffuser structure in order to capture any discharge-related trends in seawater properties. Six of the stations lie along a north-south axis at the same water depth (15.2 m) as the center of the diffuser. Stations 3 and 4 are positioned at the upcoast and downcoast boundaries of the ZID, at a distance of 15 m from the closest diffuser ports (Table 1). Stations 2 and 5 are located at nearfield distances (60 m) from the diffuser centroid. Stations 1 and 6 represent midfield stations, and are situated 100 m upcoast and downcoast of the centroid. Depending on the direction of the local oceanic currents at the time of sampling, one or more of these stations could conceivably be influenced by the discharge. Under those circumstances, the midfield station on the opposite side of the diffuser can act as a reference station. Comparisons of water properties at these antipodal stations quantify departures from ambient seawater properties so that compliance with the NPDES discharge permit can be evaluated.

Table 1. Description of Receiving-Water Monitoring Stations

Station	Description	Latitude	Longitude	Closest Approach Distance ¹ (m)	Center Distance ² (m)
1	Upcoast Midfield	35° 23.253' N	120° 52.504' W	88.4	100
2	Upcoast Nearfield	35° 23.231' N	120° 52.504' W	49.4	60
3	Upcoast ZID	35° 23.210' N	120° 52.504' W	15.0	20
4	Downcoast ZID	35° 23.188' N	120° 52.504' W	15.0	20
5	Downcoast Nearfield	35° 23.167' N	120° 52.504' W	49.4	60
6	Downcoast Midfield	35° 23.145' N	120° 52.504' W	88.4	100
7	Offshore Midfield	35° 23.199' N	120° 52.570' W	85.8	100
8	Offshore Nearfield	35° 23.199' N	120° 52.544' W	46.7	60
9	Offshore ZID	35° 23.199' N	120° 52.519' W	15.0	23
10	Shoreward ZID	35° 23.199' N	120° 52.489' W	15.0	23
11	Shoreward Nearfield	35° 23.199' N	120° 52.464' W	46.7	60
12	Shoreward Midfield	35° 23.199' N	120° 52.438' W	85.8	100
13	Southwest Nearfield	35° 23.176' N	120° 52.532' W	59.8	60
14	Northwest Nearfield	35° 23.222' N	120° 52.532' W	40.2	60
15	Northeast Nearfield	35° 23.222' N	120° 52.476' W	59.8	60
16	Southeast Nearfield	35° 23.176' N	120° 52.476' W	40.2	60

¹Distance to the closest open diffuser port.

²Distance to the center of open diffuser section.

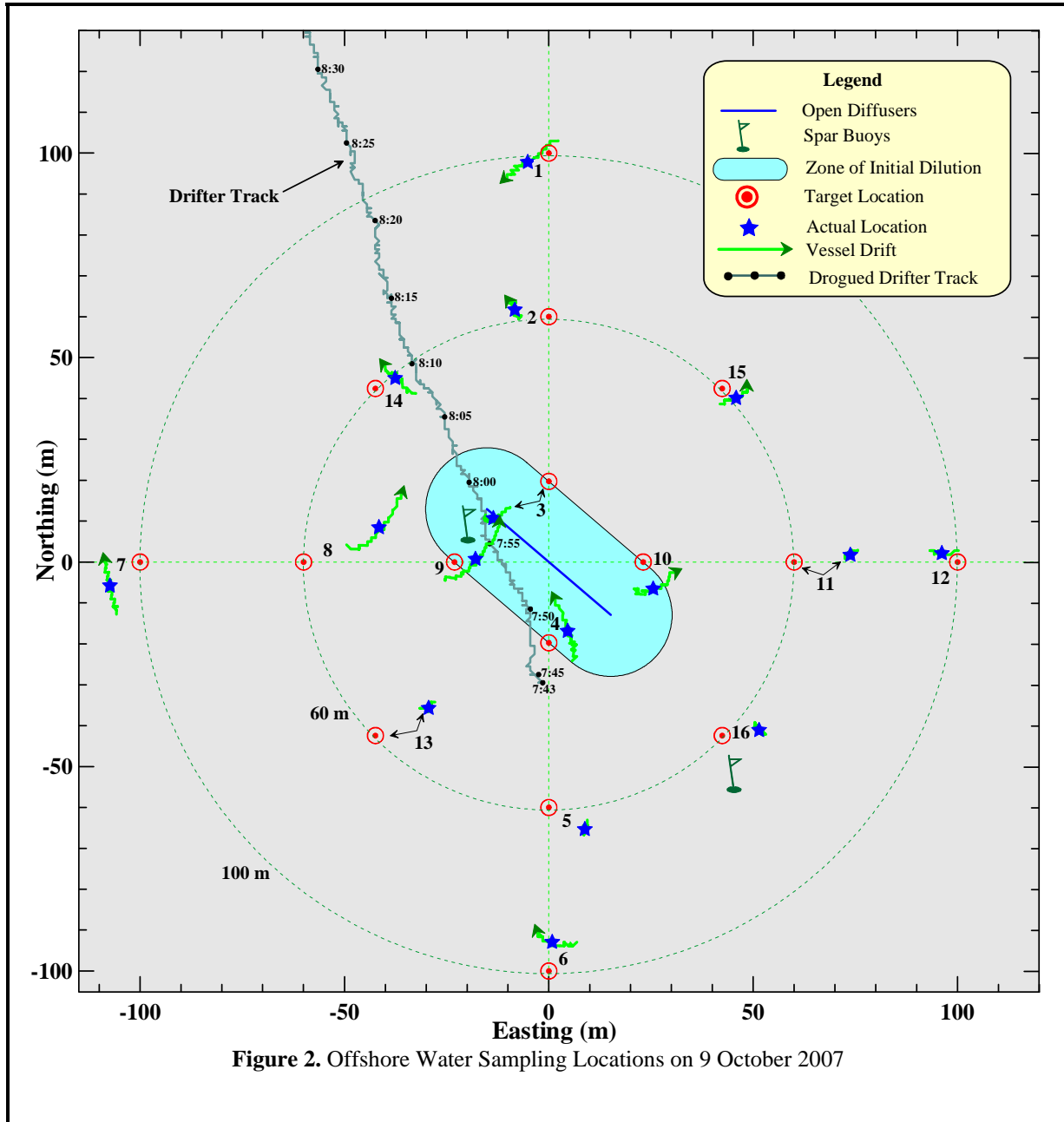


Figure 2. Offshore Water Sampling Locations on 9 October 2007

Six other stations (7 through 12) are aligned along a cross-shore transect in a pattern matching that of the along-shore transect. The remaining four stations (13 through 16) measure the nearfield influence of effluent transported by ocean currents flowing at oblique angles to the bathymetry.

An important consideration in the assessment of wastewater dispersion close to the discharge is the finite size of the diffuser. Although the discharge is considered a ‘point source’ for modeling and regulatory purposes, it does not occur at a point of infinitesimal size. Instead, the discharge is distributed along a 42 m section of the seafloor. Because of this distributed discharge, the amount of wastewater dispersion at a given point in the water column is dictated by its distance to the closest diffuser port, rather than its

distance to the center of the diffuser structure. The ‘*closest approach*’ distance can be considerably less than the centerline distance normally cited in modeling studies (Table 1).

Another important consideration for compliance evaluation is the ability to determine the actual location of the measurements. The ability to discern small spatial separations among stations within the compact sampling pattern specified in the discharge permit became feasible only after the advent of DGPS. The accuracy of traditional navigation systems such as LORAN or standard GPS is typically ± 15 m, a span equal to half the total width of the ZID itself. Prior to 2 May 2000, standard commercial GPS receivers were not allowed to be perfectly accurate by law; and a built-in error system called Selective Availability (SA) was encoded into GPS transmissions. SA could introduce a misreading of up to 100 m, although it altered most measurements by less than 30 m. After May 2000, SA was turned off, and the accuracy of standard GPS receivers improved substantially, with horizontal position errors that are now typically less than 10 m.

Even so, extreme atmospheric conditions and physiographic obstructions can still cause satellite signals to bounce around, leading to errors in position beyond those that were previously introduced by SA. These other errors are greatly reduced with the Differential GPS (DGPS) system that was first implemented by the U.S. Coast Guard to enhance offshore navigation. DGPS incorporates a second signal from a nearby, land-based beacon. Because the beacon is fixed at a known location, the position error in the reading from the GPS satellites can be precisely calculated at any given time. This correction is continuously transmitted to the DGPS receiver onboard the survey vessel and provides an extremely stable and accurate offshore navigational reading, typically with position errors of less than 2 m.

At the beginning of 1998, the survey vessel F/V *Bonnie Marietta* was fitted with a Furuno™ GPS 30 and FBX2 differential beacon receiver. This navigational system was used on 29 July 1998 to precisely locate the position of the open section of the diffuser structure (MRS 1998b) and establish the new target locations for the receiving-water monitoring stations shown in Figure 2 and listed in Table 1. The survey vessel is now fitted with two independent DGPS receivers to allow access to two separate land-based beacons for navigational intercomparison, which ensures extremely accurate and uninterrupted navigational reports.

Frequent recording of DGPS readings allows precise determination of sampling locations throughout the vertical CTD profiling at individual stations. Knowledge of the precise location of individual CTD measurements relative to the diffuser position is crucial for accurate interpretation of the water-property fields. During any given survey, the actual sampling locations rarely coincide with the exact target coordinates listed in Table 1. Winds, waves, and currents induce offsets during sampling. Equally important are the offsets caused by the residual momentum of the survey vessel as it approaches the target locations. Using DGPS, these offsets can be resolved and the vessel location can be precisely tracked throughout sampling at each station. This is an important consideration because vertical profiling conducted at an individual station can cover a large horizontal distance relative to the ZID.

The magnitude of the horizontal drift that occurred at each of the stations during the October 2007 survey is apparent from the length of the green tracklines in Figure 2. These tracklines trace the horizontal location of the CTD instrument package as it is lowered to the seafloor. Their lengths reflect the station-keeping difficulty experienced during the October 2007 survey. During the time it took the CTD to traverse the water column to the seafloor, which averaged 1 min 30 s, the instrument package moved as much as 19.3 m laterally. Overall, however, the drift was only 9.4 m when averaged over all the stations. This amount of drift is fairly typical of most surveys.

The CTD trajectories reflect the complex interaction between surface currents, wind forces, and residual momentum as the vessel approached each station. Generally, winds can move the vessel to a greater degree than current flow. However, as summarized in Table B-9, winds were light and variable during the survey. As a result, their influence was minimal compared to the northward drift induced by the prevailing current. As shown by the green tracklines in Figure 2, the drift at many of the stations had a northward component. At Stations 1 and 3, the apparent southward drift of the CTD was induced by residual momentum left after the vessel approached the station from the north. The influence of vessel momentum was apparent in the vessel tracklines recorded before each downcast was conducted. Although these portions of vessel tracks are not shown in Figure 2, the approach directions were consistent with that of the vessel drift recorded throughout each CTD cast.

Although small compared to the survey vessel's length, drift in the CTD location during the downcasts complicates the assessment of compliance with discharge limitations at stations close to the diffuser structure. Receiving-water limitations specified in the COP only apply to measurements recorded beyond the ZID boundary. Within the ZID, rapid turbulent mixing associated with the momentum of the effluent jet and the rise of the buoyant plume is expected, and the limitations apply to conditions after this initial mixing is complete. Specifically, during the October 2007 survey, the vertical profiles at Stations 9 and 10 traversed the boundary of the ZID (Figure 2). Thus, strictly speaking, only a portion of the data recorded during these casts were subject to the receiving-water limitations specified in the NPDES discharge permit. Additionally, none of the measurements recorded at Stations 3 or 4 were subject to the limitations because the CTD was well within the ZID boundary throughout the entire vertical cast at those stations.

Compliance assessments notwithstanding, measurements recorded close to the diffuser structure within the ZID lend valuable insight into the outfall's effectiveness at dispersing wastewater during the October 2007 survey. Damaged or broken diffuser ports would be reflected by low dilution rates and measurements of concentrated effluent throughout ZID. Without measurements recorded within the ZID, the discharge plume might go undetected. This was the case in nearly every water-quality survey conducted prior to 1999, before the denser sampling pattern that is now in use was instituted.

Surveys prior to 1999 also predated the advent of DGPS. Consequently, the 9.4 m average drift experienced during sampling at individual stations in the October 2007 survey would not have been resolved with the navigation available prior to 1999. In fact, before 1999 sampling was presumed to occur at a single, imprecisely determined, horizontal location near each station. Federal and State reporting of monitoring data still depends on identification of a single position for all of the CTD data collected at a particular station. Thus, for regulatory reporting, and for historical consistency with past surveys, a single sampling location was also reported for each station during the October 2007 survey. These positions were based on the average locations shown for each station by the blue stars in Figure 2. The average positions are also listed in Table 2, along with their distance from the diffuser structure. However, based on the foregoing discussion, an average station position that happens to lie within the ZID does not imply that none of the measurements collected at that particular station were subject to the receiving-water objectives in the discharge permit.

For example, the hydrocast at Station 9 began outside of the ZID boundary, as shown by the start of the green arrow in Figure 2. As such, these shallow measurements would be subject to receiving-water limitations even though the average Station 9 location was well within the ZID. Moreover, the average 10.9-m distance listed in Table 2 lends little insight into the true proximity of the measurements relative to the discharge. As the CTD was lowered into the water column at Station 9, it drifted 19.3 m toward the northeast, where it passed within 53 cm of the diffuser structure before reaching the seafloor on the opposite side of the ZID. The closest-approach distance of 10.9 m that is listed for Station 9 was based on

Table 2. Average Coordinates of Vertical Profiles during the October 2007 Survey

Station	Time (PDT)		Latitude	Longitude	Closest Approach	
	Downcast	Upcast			Range ¹ (m)	Bearing ² (°T)
1	7:55:23	7:57:11	35° 23.252' N	120° 52.507' W	85.6	7
2	7:59:54	8:01:25	35° 23.232' N	120° 52.510' W	49.4	8
3	8:03:58	8:05:47	35° 23.205' N	120° 52.513' W	0.5 ³	41
4	8:10:30	8:12:11	35° 23.190' N	120° 52.501' W	9.7 ³	221
5	8:15:19	8:16:47	35° 23.164' N	120° 52.498' W	52.6	187
6	8:22:12	8:23:47	35° 23.149' N	120° 52.503' W	81.1	190
7	8:32:18	8:33:51	35° 23.196' N	120° 52.575' W	94.1	259
8	8:37:35	8:39:13	35° 23.204' N	120° 52.531' W	26.7	261
9	8:41:51	8:43:19	35° 23.200' N	120° 52.516' W	10.9 ⁴	221
10	8:46:46	8:48:04	35° 23.196' N	120° 52.487' W	12.3 ⁴	58
11	8:51:40	8:52:53	35° 23.200' N	120° 52.455' W	60.5	76
12	8:57:13	8:58:40	35° 23.200' N	120° 52.440' W	82.4	79
13	8:28:14	8:29:39	35° 23.180' N	120° 52.523' W	46.1	221
14	9:09:26	9:10:52	35° 23.223' N	120° 52.529' W	39.3	325
15	9:05:28	9:06:46	35° 23.221' N	120° 52.474' W	60.4	41
16	9:01:29	9:02:56	35° 23.177' N	120° 52.470' W	45.8	128

¹ Distance from the closest open diffuser port to the average station position. Stations with some observations collected within the ZID are shown in bold.

² Direction measured clockwise in degrees from true north from the closest diffuser port to the average sampling location.

³ All of the CTD cast was within the ZID boundary.

⁴ Portions of the CTD (Conductivity-Temperature-Depth) cast were within the ZID boundary.

the average of surface and bottom position fixes measured at the beginning and end of the downcast. The resulting average position, which is shown by the blue star in Figure 2, would suggest that all the data at Station 9 were collected well away from the diffuser, at a location near the edge of the ZID where initial dilution would be expected to have been completed.

A satellite-tracked drifter documented the prevailing north northwestward flow during the October 2007 survey. As in past reports, its trajectory is shown by the grey line with black dots in Figure 2. The drifter is designed to track the subsurface current, with little influence from the wind. Each dot along the drifter trackline represents a time span of five minutes. The drogued drifter was deployed near Station 4 at 07:43 PDT. The drifter was recovered an hour and thirty-three minutes later, at 09:16 PDT. In contrast to most other surveys, the moderately strong current rapidly carried the drifter out of the survey area. Its subsequent movement is presented in Figure 3. The trajectory shows that throughout its deployment, the drifter's movement was comparatively constant in both speed and direction, possibly because the tidal forcing was consistent throughout the survey (Figure 4). The drifter did, however, respond to a brief, ten minute, weakening of the westward drift component between 08:45 PDT and 08:55 PDT, after which it resumed its original trajectory toward the north northwest. During its overall deployment, the drifter traversed 368 m toward the north northwest (344°T) at an average speed of 6.65 cm/s or 0.13 knots.

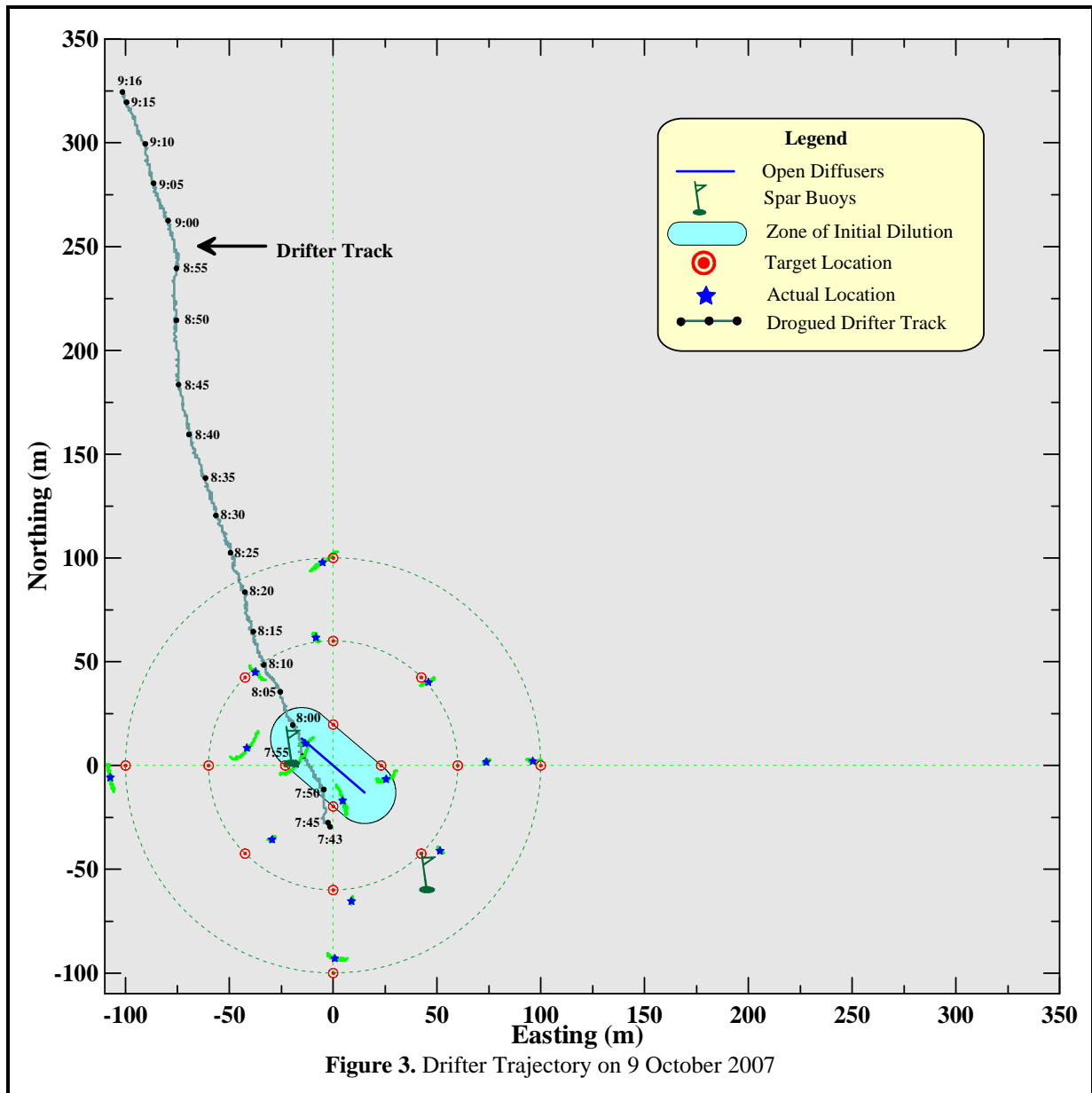
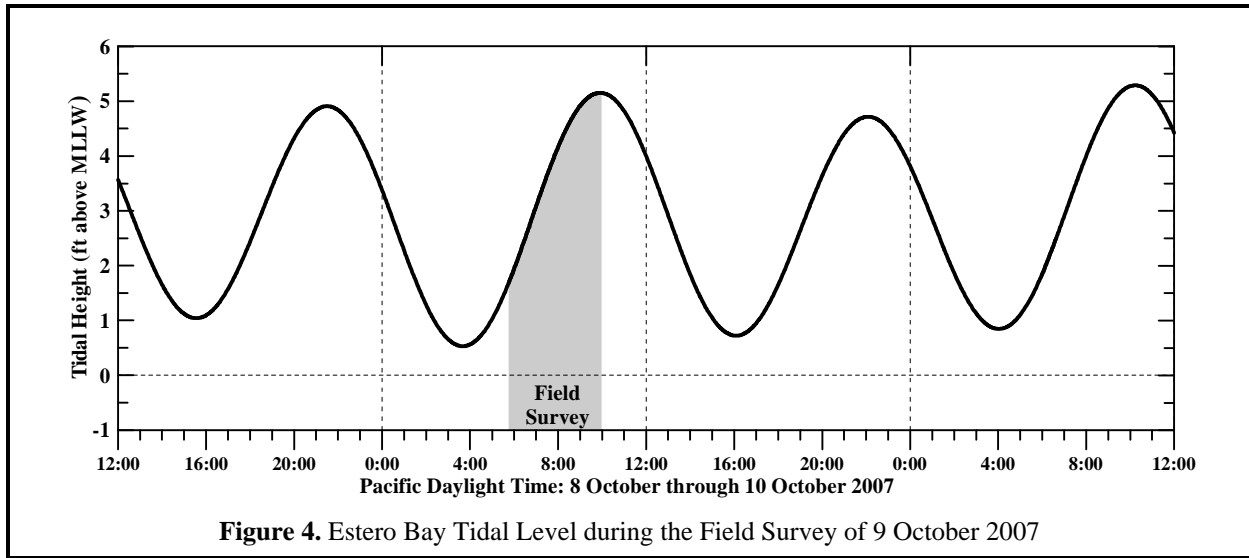
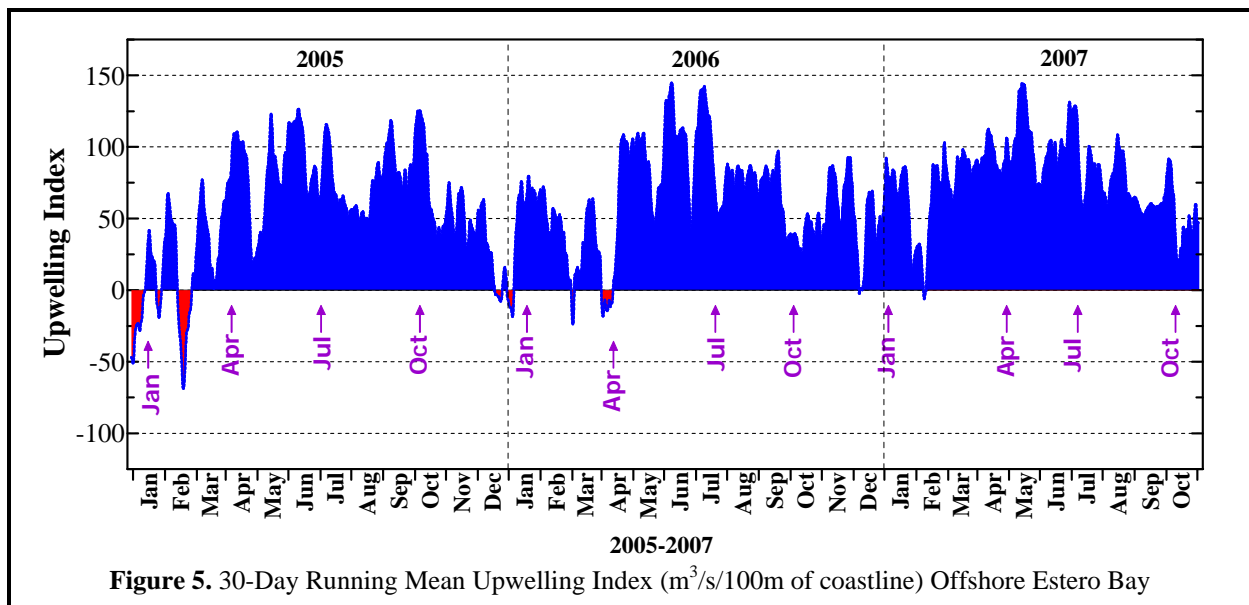


Figure 3. Drifter Trajectory on 9 October 2007

The northward flow component that was measured by the drogued drifter was consistent with the incoming (flood) tide that prevailed during the survey (Figure 4). Flow is often heavily influenced by external processes, such as wind-generated upwelling or by passing offshore eddies. For example, upwelling normally induces an offshore-directed surface flow toward the south southwest. Figure 5 shows, however, that the unusually persistent and intense upwelling conditions that prevailed throughout most of 2007 declined markedly around the time of the October survey. In the absence of these external influences, a flood tide induces a weak northeastward flow in the survey region. During the October 2007 survey, the flood tide resulted in a northward directed flow, however, the slight westward trend reflects the influence of the mild upwelling conditions that were also present at the time.



The mild upwelling conditions that prevailed at the time of the survey are reflected in the distribution of sea surface temperatures measured by infrared sensors on one of NOAA’s polar orbiting satellites. The surface temperature distribution on the day prior to the survey is shown on the cover of this report. At that time, skies were clear enough for sea-surface temperatures to be recorded without interference from cloud cover. The satellite image depicts slightly cooler surface seawater temperatures within Estero Bay that were generated by mild upwelling conditions. The mild upwelling was responsible for the weak water-column stratification that is evident in the vertical profiles collected with the CTD (Figures A-1 through A-3 in Appendix A). Figure 5 shows that the upwelling season normally begins sometime during late March and or early April when there is a “spring transition” to more persistent southward-directed winds along the Central California Coast. This transition is marked by the stabilization of a high atmospheric pressure field over the northeastern Pacific Ocean. Clockwise winds around this pressure field drive the prevailing northwesterly winds along the Central Coast. These prevailing winds move surface waters



southward and offshore. To replace these coastal surface waters, deep, cool, nutrient-rich waters upwell near the coast.

In early October 2007, the temporary relaxation of these sustained southeastward-directed winds resulted in milder upwelling conditions and sea surface temperatures close to the coastline that were not as cold as during prior months. Nevertheless, the satellite image on the cover depicts the presence of slightly cooler, upwelled water within Estero Bay, with temperatures at or below 13°C, in dark blue. The Estero Bay surface waters were approximately 1°C cooler than the seawater along much of the south-central coast. The image also depicts another characteristic of upwelling, wherein jets of cooler coastal water extend offshore at major promontories, such as Point Piedras Blancas. These jets are generally more pronounced when upwelling conditions are stronger, but are still identifiable in the October 2007 image as fingers of dark blue extending offshore. These features reflect the offshore transport of cool surface waters that were upwelled near the coast. Farther offshore and to the south, surface water temperatures were as much as six degrees warmer, as delineated by the areas with yellow and orange shading. The cooler upwelling-induced temperatures present in Estero Bay, where the October 2007 survey was conducted, were consistent with the near-surface temperatures measured by the CTD during the survey, which averaged 12.96°C (Table B-1 in Appendix B),

The nutrient-rich seawater that is brought to the sea surface by upwelling enables phytoplanktonic blooms that are the foundation of the productive marine fishery found along the California coast. The cross-shore flow associated with persistent upwelling conditions also leads to vertical stratification of the water column. The resulting shallow (<10 m) thermocline is commonly maintained throughout the summer and into the fall. During the October 2007 survey, the mild character of the upwelling conditions resulted in only a weak thermocline. Nonetheless, the observed vertical stratification was still much larger than what normally occurs during winter. In winter, vertically uniform conditions result from water-column mixing generated by intense winds generated by passing storm fronts, and large waves produced by distant Pacific storms. Northwestward winds behind these storm fronts can even induce downwelling, which further deepens the mixed layer. Figure 5 shows that most of these downwelling events occur before May, at least in 2005 and 2006. Downwelling events, which are measured by negative downwelling indices, are highlighted in red in the Figure. In contrast to normal conditions, the winter months at the beginning of 2007 had only one, very minor, northwestward wind event, which was accompanied by weak downwelling.

METHODS

The 38 ft F/V *Bonnie Marietta*, owned and operated by Captain Mark Tognazzini of Morro Bay, served as the survey vessel on 9 October 2007. Dr. Douglas Coats of Marine Research Specialists (MRS) was the Chief Scientist while Captain Mark Tognazzini supervised vessel operations and Mr. William Skok acted as marine technician. Ms. Bonnie Luke and Mr. Tyler Eck, both of MRS, provided additional scientific support and collected auxiliary measurements of meteorological and oceanographic conditions throughout the survey. These included Secchi depth measurements and standard observations for weather, sea conditions, and water clarity/coloration as recorded in Table B-9. Wind speeds and air temperatures were measured with a Kestrel[®] 2000 Thermo-Anemometer. These auxiliary observations were collected contemporaneously with the rapid water-column profiling that was conducted at each station using a CTD instrument package.

Auxiliary Measurements

At all stations, a Secchi disk was lowered through the water column to determine its depth of disappearance (Table B-9). Secchi depths provide a visual measure of near-surface turbidity or water clarity. The depth of disappearance is inversely proportional to the average amount of organic and inorganic suspended material along a line of sight in the upper water column. As such, the Secchi depth measures natural light penetration, which can be limited by increased suspended particulate loads from plankton blooms, onshore runoff, seafloor resuspension, and wastewater discharge. It is also of biological significance because the depth of the euphotic zone, where most oceanic photosynthesis occurs, extends to approximately twice the Secchi depth. Secchi depths varied between 6.5 m and 8 m during the October 2007 survey, reflecting the presence of a euphotic zone that extended to depths greater than 13 m, and reached the seafloor at some stations. A euphotic zone that is limited to the upper reaches of the water column is typical of upwelling conditions when increased primary production, namely, increased phytoplankton density, decreases the transmission of ambient light through the near-surface mixed layer. However, due to the mild upwelling conditions during the October survey, the euphotic zone extended to greater depths than in the last two surveys when stronger upwelling conditions limited photosynthesis to depths less than 9.5 m.

Secchi depths provide less precise measures of light transmittance than the transmissometer mounted on the CTD instrument package. For example, the visibility of the disk, and hence its depth of disappearance, depends on the amount of natural light available at the time of the measurement. Thus, the Secchi depth reading can artificially change by as much as 0.5 m depending on whether the sample is taken on the sunny or shady side of the survey vessel. To minimize the influence of variations in ambient light, the Secchi depth measurements were collected in a consistent manner throughout the survey. Nevertheless, temporal drift in the measurements can be introduced as the sun rises in the sky, or as cloud cover changes as the survey progresses. Neither of these influences were particularly evident during the October 2007 survey, so the Secchi depth measurements accurately reflect general turbidity levels within the upper portion of the water column. This includes waters within a meter of the sea surface where, because of the physical size of the CTD package, the transmissometer cannot record turbidity.

During the October 2007 survey, a satellite-tracked drifter was deployed near the open section of the diffuser structure. The drifter was drogued at mid-depth (7 m) using the curtain-shade design of Davis et al (1982). In this configuration, the drifter's trajectory was largely dictated by the oceanic flow field rather than by surface winds. The times and precise positions of the drifter deployment and recovery were recorded to determine the overall strength and direction of plume transport during the October 2007 sampling effort. In addition, the October 2007 survey was the eleventh MBCSD survey to record the drifter position throughout its deployment, rather than merely calculating the average flow velocity solely from the vessel position at the time of the drifter's deployment and recovery.

Instrumental Measurements

Vertical water-column profiling was conducted using an electronic instrument package equipped with a number of probes and sensors. A Sea Bird Electronics SBE-19 Seacat CTD package was used to collect profiles of conductivity, salinity, temperature, light transmittance, dissolved oxygen (DO), pH, density, and pressure at each station. A submersible pump on the CTD continuously flushed water through the conductivity cell and oxygen plenum at a constant rate, independent of the CTD's motion through the water column. After the October 2001 survey, the CTD was returned to the factory for full testing, repair, and calibration. Temporal drifts in the oxygen and alkalinity readings during the October 2001 survey indicated that the sensitivity of these probes had degraded because of an accumulation of marine growth.

During the factory repair, both the pH probe and the electrolyte in the oxygen sensor were replaced. The entire CTD system was then calibrated at the factory. Upon return of the instrument, the transmissivity, dissolved oxygen, and pH sensors were recalibrated at the MRS laboratory. Calibration coefficients determined at the factory and by MRS were nearly identical, and confirmed the accuracy and stability of the refurbished sensors.

The DO and pH sensors were again returned to the factory in May 2003 and in June 2006 for testing and calibration. Because of increasing temporal drift associated with the aging DO probe, it was replaced on both occasions with a new DO probe. As is the case before all surveys, the CTD system was recalibrated at the MRS laboratory prior to the October 2007 survey. Calibration at upper-bound DO concentrations was established by immersing the CTD in an aerated, temperature-controlled calibration tank. In addition to oxygen readings at full saturation, a zero-oxygen calibration point was determined by filling the oxygen-sensor plenum with an 8% solution of sodium sulfite (Na₂SO₃). Oxygen calibration coefficients were determined by regression analysis of sensor-membrane current and temperature, as recommended by the manufacturer (SBE 1993). As with prior factory calibrations, pre-cruise calibration coefficients determined by MRS closely corresponded to those determined by the factory.

The six seawater properties that were used to assess receiving-water quality in this report were derived from the continuously recorded output from the probes and sensors on the CTD. Pressure housing limitations on the combination oxygen/pH sensor confine the CTD to depths less than 200 m (Table 3), which is well beyond the maximum depth of the deepest station in the outfall survey. The precision and accuracy of the various probes, as reported in manufacturer's specifications, are also listed in Table 3. Salinity (‰) was calculated from conductivity (Siemens/m) measurements. Density was derived from contemporaneous temperature (°C) and salinity data. It was expressed as 1000 times the specific gravity minus one, which is a unit of sigma-T (σ_t).

Table 3. Instrumental Specifications for CTD Profiler

Component	Depth¹	Units	Range	Accuracy	Resolution
Housing	600	—	—	—	—
Pump	3400	—	—	—	—
Pressure	680	Psia	0 to 1000	± 5.0	± 0.5
Depth	—	Meters	0 to 690	± 3.0	± 0.3
Conductivity	600	Siemens/m	0 to 6.5	± 0.001	± 0.0001
Salinity	600	‰	0 to 38	± 0.006	± 0.0006
Temperature	600	°C	-5 to 35	± 0.01	± 0.001
Transmissivity	2000	%	0 to 100	± 0.1	± 0.025
Dissolved Oxygen	200	mg/L	0 to 21.5	± 0.14	± 0.014
Acidity/Alkalinity	200	pH	0 to 14	± 0.1	± 0.006

¹ Maximum depth limit in meters

All three of these physical parameters (salinity, temperature, and density) were used to determine the lateral extent of the effluent plume. Additionally, they quantified the layering, or vertical stratification and stability of the water column, which determines the behavior and dynamics of the wastewater as it mixes with seawater within the ZID. Data on three remaining seawater properties, consisting of light transmittance (water clarity), hydrogen-ion concentration (acidity/alkalinity – pH), and dissolved oxygen (DO), further characterized receiving waters, and were used to assess compliance with water-quality criteria. Light transmittance was measured as a percentage of the initial intensity of a transmitted beam of

light detected at the opposite end of a 0.25 m path. Increased transmittance indicates increased water clarity and decreased turbidity.

During the pre-cruise calibration, coefficients for the pH (alkalinity) sensor were determined from a linear regression of output voltage after immersion in three separate buffered solutions of known pH. Buffering solutions with a pH of 4 ± 0.01 , 7 ± 0.01 , and 10 ± 0.02 were used to bracket the range of in situ measurements. The SeaTech transmissometer was air calibrated by fitting the voltages recorded with and without blocking of the light transmission path in air, as recommended by the manufacturer (SBE 1989). Revised calibration coefficients determined prior to the survey were used in the algorithms that converted sensor voltage to engineering units when the field data were processed. Comparison with the factory calibration of the entire CTD package that was conducted in December 2001, and the more recent June 2006 replacement and calibration of the DO probe, confirmed the continued accuracy and stability of the temperature, pressure, and conductivity sensors, as well as the operational integrity of the oxygen and pH probes.

Before deployment at the initial station, the CTD was held below the sea surface for a six-minute equilibration period. Subsequently, the CTD was raised to within 1.0 m of the sea surface and profiling commenced. The CTD was lowered at a continuous rate of speed to the seafloor. Measurements at all the stations were collected during single deployment of the CTD package by towing it below the water surface while transiting between adjacent stations. Upon retrieval of the CTD, the profile data were downloaded to a portable computer and examined for completeness and range acceptability.

Temporal Trends in the DO and pH Sensors

The DO and pH sensors exhibited temporal drift during the October 2007 survey. Perceptible drift in pH measurements has been consistently observed in prior water-quality surveys as the result of ongoing sensor equilibration during profiling. The very small drift in the DO sensor is normally imperceptible except during surveys when the range in the ambient DO field is small, as was the case during the October 2007 survey. For the pH sensor, prolonged exposure to the atmosphere between surveys results in the largest offsets and can also affect the dynamic range of the measurements. During past surveys, smaller equilibration offsets were also observed when the CTD was redeployed after being brought onboard to download data during the middle of the survey. Use of a single deployment during the October 2007 survey obviated the need for mid-survey adjustments for pH drift.

Previous additional attempts to mitigate sensor drift have included prolonging the soak time of the CTD prior to profiling. Soak times of six minutes at the beginning of a survey were found to reduce, but not entirely eliminate sensor drift. During other surveys, a tube filled with seawater was placed around the pH sensor while in transit to the survey site to limit atmospheric exposure of the probe prior to deployment. This technique has been successful at further ameliorating sensor drift. A suitable tube was not available during the October 2007 survey, however, which may explain why the observed pH drift was slightly larger than in other surveys conducted this year.

Temporal drift in the DO and pH sensors was responsible for slight, but perceptibly lower measurements at stations occupied during the initial stages of the CTD deployment. Beginning with Station 1, where the respective DO and pH offsets were -0.60 mg/L and -0.068 pH units, equilibration-related reductions became steadily smaller as the survey progressed sequentially from Station 2 (-0.39 mg/L and -0.046 pH) through Station 9. The magnitude of the offsets at each station was determined by comparing values

recorded near the seafloor at a given station with values measured toward the end of the survey after Station 9, when the sensors had fully equilibrated.

Removal of the artificial DO and pH trends was important because the drifts were large compared to reported accuracy and precision of the probes. As a result, they could potentially mask very slight discharge-related anomalies. The artificial pH reduction (-0.068 pH) at the beginning of the deployment was significantly larger than the instrumental resolution (± 0.006 pH) reported by the probe manufacturer (Table 3). Similarly, the artificial DO reduction (-0.60 mg/L) at Station 1 was significantly larger than the reported accuracy of the DO probe (± 0.14 mg/L). Before correction, equilibration-related offsets induced an artificial lateral gradient in the along-shore transect which appears in Tables B-7 and B-8 as a statistically significant reduction in DO and pH at Stations 1 and 2. As shown in Tables B-4 and B-6, temporal detrending effectively removed the artificial gradients in the DO and pH fields and eliminated erroneous anomalies that were unrelated to the true spatial distributions present at the time of the survey.

RESULTS

The fourth-quarter water-quality survey began on Tuesday, 9 October 2007, at 07:43 PDT with the deployment of the drogued drifter. Subsequently, water-column measurements were collected as required by the NPDES monitoring program (Table 2 and B-9). Sunrise was at 07:04 PDT and skies were largely overcast throughout the survey, which ended at 09:16 PDT with the retrieval of the drogued drifter.

Light and variable winds prevailed throughout the survey (Table B-9). Average wind speeds, calculated over one-minute intervals, ranged from 1.0 kt to 3.7 kt, with peak speeds ranging from 1.8 kt to 6.6 kt. Additionally, a 1 to 2 ft swell moved through the survey area from the west. Atmospheric visibility was greater than 2 nM along the ocean surface owing to the absence of low-lying fog. As a result, Morro Rock and the shoreline remained visible throughout the survey. Air temperatures remained relatively constant at 10.4°C during the first part of the survey until around 09:00 PDT, when insolation from the rising sun warmed the atmosphere by approximately 1°C. As a result of its limited accuracy, the average surface seawater temperature of 11.7°C measured by a hand-held infrared sensor (Table B-9) was approximately 1°C lower than the average temperature recorded by the CTD (12.96°C in Table B-1) and recorded by the satellite as shown on the cover of this report.

The discharge plume was not visible near the sea surface at any time during the survey. Throughout the survey, there was also no visual evidence of floating particulates, oil and grease, or seawater discoloration associated with the discharge.

Beneficial Use

During the October 2007 survey, observations of beneficial use demonstrated that the coastal waters within Estero Bay continued to be utilized by wildlife and for recreation. California brown pelicans (*Pelecanus occidentalis californicus*), Pelagic cormorants (*Phalacrocorax pelagicus*), Brandt's cormorants (*Phalacrocorax penicillatus*), Heermann's gulls (*Larus heermanni*), and western gulls (*Larus occidentalis*) were observed during transit to and from the survey area, and throughout the course of the survey. During a portion of the survey, a western gull was observed perched atop one of the spar buoys that marks the location of the diffuser structure.

In addition to bird life, a several species of marine mammals were also observed during the survey. Both southern sea otters (*Enhydra lutris*) and California sea lions (*Zalophus californianus*) were observed

during transit to the survey site, as well as foraging near the outfall during the survey itself. Additionally, a harbor porpoise (*Phocoena phocoena*) was observed just outside of the surfzone during the survey. Pieces of detached bull kelp (*Nereocystis luetkeana*) were also noted drifting in the survey area and during transit to the survey area.

Several vessels were observed during the course of the survey, including three small commercial fishing boats, which left the bay before transiting to locations further offshore to the north. Numerous pedestrians were seen walking along Atascadero Beach during the survey. Additionally, one surfer was observed in the water close to Morro Rock and two kayakers were seen just outside of the surfzone to the northeast of the survey area.

Ambient Seawater Properties

Data collected during the October 2007 survey reflect weakly stratified conditions that are indicative of mild upwelling conditions. Upwelling results in an influx of dense, cold, saline water at depth and often leads to a sharp thermocline, halocline, and pycnocline where temperature, salinity, and density change rapidly over short vertical distances. Under heavily stratified conditions, isotherms crowd together to form a thermocline that restricts the vertical transport of the effluent plume and reduces its dispersion.

In contrast to the sharply defined stratification characteristic of intense upwelling, only weak upwelling-induced vertical gradients were evident throughout the water column during the October 2007 survey as shown in the vertical profiles of Figures A-1 through A-3. Also, the vertical range in the upwelling induced gradient is of a much smaller magnitude than that found when strong upwelling conditions prevail. For example, the vertical profiles show that the difference between seafloor and sea surface temperatures during the October 2007 survey was less than 1°C. In contrast, the more intense upwelling conditions present during the April and July 2007 surveys, resulted in vertical temperature differences that were twice as large, and occurred over a smaller depth interval.

Nevertheless, an upwelling-induced thermocline, where temperature steadily decreases with increasing depth, is evident in all but one of the vertical profiles shown in Figures A-1 through A-3 (red lines) for the October 2007 survey. In contrast to the broad temperature change seen at most stations, the vertical temperature change at Station 2 was largely restricted to a narrow depth region between 2 m and 3.5 m (top right frame of Figure A-1). As described in the following sections, the presence of the effluent discharge plume altered the vertical structure of the water column at that station.

Other ambient seawater properties also exhibited a weak vertical structure that was indicative of upwelling-induced stratification. For example, the shape of the temperature profile at most stations was reflected in the profiles of dissolved oxygen (dark blue lines), and to a lesser extent, in the profiles of pH (olive-colored lines). Similarly, the general decrease in temperature, DO, and pH with depth are mirrored by a pycnocline where density (black lines) steadily increases with depth below approximately 5 m. Thus, upwelling-induced stratification dictated the vertical structure of all ambient seawater properties except salinity (green lines) and transmissivity (light-blue lines).

DO concentrations were highest within the 5 m deep, surface mixed layer where atmospheric equilibration and upwelling-induced photosynthesis saturated the seawater with oxygen. Near the sea surface, direct, gaseous exchange with the overlying atmosphere combined with increased primary productivity to produce higher DO concentrations. Also, nutrient-rich seawater brought to the sea surface by upwelling enabled phytoplanktonic blooms that produced oxygen and consumed carbon dioxide (CO₂). The associated increase in planktonic biomass within the surface mixed layer resulted in the

slightly reduced water clarity that is evident in many of the vertical profiles of light transmittance (light-blue lines in Figures A-1 through A-3). As the ratio of respiration to photosynthesis increased with depth below the mixed layer, there was an increase in dissolved CO₂ (carbonic acid) and a concomitant decline in pH, reflecting the slightly more acidic nature of the seawater. These biological processes account for the decline in pH (olive-colored lines) with increasing depth that is apparent in most of the vertical profiles.

Cross-shore transport associated with upwelling also influenced the vertical distribution of seawater properties. Near the seafloor, upwelling transported cold, dense seawater onshore to replace nearshore surface waters that were driven offshore by prevailing winds. The undersaturated DO found at depth was a clear indicator of the deep offshore origin of this watermass. Deep offshore waters are undersaturated in oxygen because they have not had direct contact with the atmosphere for long periods of time, and biotic respiration and decomposition have slowly depleted the dissolved-oxygen levels. Under strong upwelling conditions, slightly elevated salinity immediately above the seafloor is indicative of waters that originate in the Southern California Bight. These saline waters are carried northward below the sea surface by the Davidson Undercurrent. In contrast, surface salinity within Estero Bay is largely influenced by the diffuse southward-flowing California Current, which represents the eastern limb of the clockwise-flowing gyre that covers much of the North Pacific Ocean. Before turning south to form the California Current, sub arctic water is carried along at high latitudes where it is exposed to high precipitation and low evaporation. As a result, the waters of the California Current are characterized by a seasonably stable low salinity (32‰ to 34‰). However, under the weak upwelling conditions of the October 2007 survey, the slightly increased salinity at depth is only apparent at some stations (green lines in Figures A-1 through A-3). At other stations, the upwelling-induced vertical salinity structure is masked by salinity spiking and, near the seafloor at Stations 3 and 9, by the presence of the low-salinity effluent plume.

In contrast to most other seawater properties, some of the variability in the vertical profiles of salinity (green lines) was caused by instrumental artifacts unrelated to natural physical oceanographic processes or effluent discharge. Often, these salinity spikes overwhelm the naturally occurring subtle increase in salinity with depth. The spikes occur in conjunction with localized sharp vertical changes in temperature, such as can be seen near 7 m at Station 14 (upper right frame of Figure A-3) and near 8 m at Station 15 (lower left frame of Figure A-3). Salinity spikes are instrumental artifacts arising from the mismatch between conductivity and temperature measurements collected near sharp, localized thermoclines. The spikes are evident as erroneous zigzag patterns, or localized salinity decreases that appear in conjunction with sharp changes in temperature. Some of the larger erroneous salinity spikes also manifest themselves in the vertical density profiles (black lines). Unless properly identified, salinity spikes can be misinterpreted as a signature of the low-salinity effluent plume. For example, the salinity spike at Station 14 was large enough to be considered a statistically significant departure from mean conditions (bolded value in Table B-2).

As with salinity spiking, some of the transmissivity measurements were erroneous sampling artifacts unrelated to actual seawater conditions that were present during the October 2007 survey. In particular, the light blue line in the lower right frame of Figure A-2 shows that unusually low transmissivity values were measured above 9 m at Station 12. Although marked reductions in transmissivity have been occasionally observed within a thin layer immediately above the seafloor known as the bottom nepheloid layer (BNLs), and similar, slight decreases within the surface mixed layer can occur due to enhanced primary production, these reductions in transmissivity are much smaller and more uniform than those recorded in the upper water column at Station 12. Localized fluctuations as large as those measured at Station 12 have not been previously observed within the upper water column in conjunction with natural oceanographic or biological processes.

However, the low transmissivity values measured at Station 12 were not likely to have been generated by the presence of effluent particulates. A 38% drop in transmissivity has never been observed in conjunction with the effluent plume, even when measured shortly after discharge. In fact, during the October 2007 survey, the CTD passed within 0.5 m of the diffuser structure during profiling at Station 9 (Figure 2) and recorded water properties within the turbulent discharge jet when very little dilution had been achieved (219:1). Even within this concentrated portion of the effluent plume, the presence of effluent particulates only reduced transmissivity by 2.2% relative to ambient levels. More importantly, Station 12 was located 100 m shoreward of the diffuser structure, in a location not likely to be influenced by the discharge given the north northwesterly transport of the effluent plume (Figure 2).

In contrast to natural processes or discharge influences, large erratic transmissivity measurements similar to those measured at Station 12 have only been observed when a piece of detached kelp or other debris temporarily became entangled on the CTD. Specifically, intermittent blockage of the light transmission path by trailing portions of the kelp fronds as the CTD descends can cause erratic drops in measured transmissivity similar to those seen in the October 2007 survey. Transmissivity readings eventually return to normal after the kelp works itself loose. Although the presence of kelp on the CTD at Station 12 was not noted at the time of the October 2007 survey, it is the likely cause of the anomalously low transmissivity measurements.

Lateral Variability

The influence of the effluent discharge can be best identified from localized anomalies in seawater properties, particularly salinity. In contrast to the isolated vertical profiles, discharge-related anomalies become especially apparent in vertical cross-sections, which highlight lateral differences in seawater properties at adjacent stations. Discharge-related anomalies are most evident near the seafloor at Stations 3 and 9 in the top frames of Figures A-4 and A-6. A discharge-related reduction in salinity was particularly large at Station 9, where measured salinities dropped below 33.6‰ due to the presence of the effluent discharge. As described above, these measurements were collected as close as 0.5 m from the diffuser structure.

By comparison, the discharge-related anomalies at Station 3 were measured no closer than 1.3 m from the diffuser structure. As a result of increased dilution across the additional 0.8 m distance, the amplitude of the salinity reduction was not as large at Station 3, and measured plume salinities were only slightly below 33.7‰. However, in contrast to the highly localized salinity anomaly at Station 9 (top frame of Figure A-6), the along-shore cross-section shown in the top frame of Figure A-4 captured the diffuse effluent plume at Stations 1 and 2 as it was transported northward by prevailing currents. Although the discharge-related reductions in salinity are readily apparent near the seafloor in the vertical profiles at Stations 3 and 9 (green lines in the middle-left frames of Figures A-1 and A-2), the subtle influence of the effluent discharge at Stations 1 and 2 only become apparent when examined in the cross-sections shown in Figure A-4. Because cross-sections provide a more useful means of tracing the effluent plume, analysis of lateral variability in seawater properties forms the basis for assessments of water-quality impacts.

The vertical cross-sections shown in Figures A-4 thru A-7 also lend insight into the mechanism that caused the discharge-related anomaly in each seawater property. The character of the salinity anomalies at Stations 1, 2, 3, and 9, as well as the density anomalies near the seafloor at Stations 3 and 9 (bottom frames of Figure A-4 and A-6), are distinctly different from spatially coincident anomalies in the other seawater properties. In particular, the localized reductions in salinity and density are vertically isolated, and appear disconnected from the surrounding, ambient seawater properties. Consequently, they could

only have been induced by the presence of dilute effluent constituents rather than the relocation of ambient seawater.

In contrast, discharge-related anomalies in other seawater properties arise because of the upward displacement of ambient seawater near the seafloor, rather than the presence of the effluent itself. For example, the mid-depth reduction in temperature at Station 2 (middle frame of Figure A-4) is apparent as an upward excursion in the 12.5°C isotherm. This thermal anomaly could not have been caused by the presence of dilute effluent because wastewater is significantly warmer than the receiving seawater upon discharge, and would manifest itself as a positive (warmer) anomaly, rather than a reduction in temperature. Instead, the mid-depth thermal anomaly was the result of ambient seawater becoming entrained in the discharge plume. This cold, deep water was carried upward into the water column by the rising plume, where it provided a perceptible contrast with the warmer surrounding seawater.

The same entrainment process generated the pH reduction observed at Station 2 (bottom frame of Figure A-5) when seawater that was naturally low in pH near the seafloor (<8.21) was transported upward by the rising discharge plume to a mid-depth location where the surrounding seawater had a higher pH (8.22). Similarly, discharge-related reductions in mid-depth transmissivity at Stations 1 and 2 (top frame of Figure A-5) were created by the upward displacement of deep seawater that had naturally low transmissivity. The upward displacement of seawater with transmissivities near 77% (delineated in green) effectively eliminated the mid-depth transmissivity maximum (>78% delineated in blue) that is apparent at the other stations.

As described above, both the entrainment-generated and the wastewater-induced anomalies become apparent when seawater properties measured at the same depth level are compared at adjacent stations. Because of this, the analysis of lateral variability in seawater properties forms the basis for assessments of water-quality impacts in this report. In particular, the significance of each potential discharge-related anomaly was statistically evaluated by comparing its amplitude to natural background variability. Each observation at a particular station was compared with the observations from other stations at the same depth level. Measurements recorded within 10 m of the sea surface were compared with other measurements at the same depth level below the sea surface. However, deeper measurements were compared with other measurements recorded at the same height above the sloping seafloor. These different depth references are used because deep seawater properties tend to parallel the sloping seafloor rather than the horizontal sea surface.

The statistical significance of departures from ambient seawater properties was computed from the raw CTD data listed in Tables B-1 through B-8. First, anomalies from mean conditions were computed by subtracting a particular measurement from the average of all other measurements at the same depth level, whether measured relative to the sea surface or the seafloor. Natural variability was then estimated from the standard deviation of all measurements (excluding the one in question) for a given seawater parameter (e.g., salinity). Statistically significant anomalies were those that departed from mean conditions by more than the 95% confidence interval, which is determined from the standard deviation and number of observations used to compute the average. Statistically significant departures from ambient conditions are highlighted in Tables B-1 through B-8 by bold typeface enclosed in boxes.

Statistically significant departures from mean conditions were found to occur in four of the six seawater properties in the October 2007 data, as shown in Table B-2 (salinity anomalies at Stations 2, 3, 9 and 14), Table B-3 (one density anomaly at 16 m at Station 9), Table B-5 (transmissivity anomalies at Stations 9 and 12), and Table B-6 (one pH anomaly at Station 2). However, only five of the eight significant anomalies were actually related to the discharge. The salinity anomalies at Stations 3 and 9 were clearly

related to the discharge largely because they were accompanied by perceptible, and in some cases statistically significant anomalies in the other seawater properties. Moreover, portions of the CTD casts at Stations 3 and 9 were in very close proximity to the outfall (Figure 4). Finally, the measured salinity within the anomalies was far lower than any salinity measured during the survey, so they could not be easily ascribed to natural variability.

The same rationale explains why the statistically significant anomalies at Stations 12 and 14 were unrelated to the discharge. First, neither station was located in the path of the discharge plume's trajectory from the diffuser structure, which is delineated by the drifter track in Figure 4. Second, Stations 12 and 14 were not in close proximity to the outfall, and the intervening Stations 4, 10, and 11, which lie closer to the outfall, did not show evidence of the discharge plume. Third, the cross-sections in Figures A-4 through A-7 do not show any evidence of anomalies in other seawater properties that coincide with the salinity anomaly at Station 14, or the transmissivity anomalies at Station 12. Discharge signatures are usually apparent in several seawater properties at once, and always in salinity.

In addition, the likely causes of the statically significant anomalies at Stations 12 and 14 were described previously, and were determined to be instrumental artifacts unrelated to the discharge or the actual seawater properties at the time of the survey. Namely, the very large transmissivity anomalies in the upper water column at Station 12 were likely caused by the intermittent blockage of the transmissometer's light path, presumably by a piece of kelp.

Similarly, the mid-depth salinity anomaly at Station 14 was an artifact of salinity spiking. Salinity spiking is a common occurrence in CTD measurements collected within upper-ocean thermoclines, and is routinely observed in MBCSD surveys conducted when the water column is stratified (MRS, 2001, 2002, 2003, 2004, 2005, 2006, 2007). Salinity spiking occurs when the CTD package crosses a strong thermocline, and the temperature and conductivity probes measure significantly different water parcels. Salinity is computed from conductivity and temperature probes that are physically separated from one another on the CTD. In addition, the sensors do not have the same response times so even if they are close together, they will not simultaneously report data from the same water parcel. Consequently, when encountering an abrupt temperature change, the mismatch between the conductivity and temperature readings results in erroneous spikes in the reported salinity. The sharper the thermal gradient, the larger the salinity spike.

The vertical profile shown in the top right frame of Figure A-3 demonstrates that this was the case for the statistically significant anomaly at Station 14. The salinity profile showed in green exhibits a classic zigzag pattern near 7 m in conjunction with several sharp changes in temperature, shown by the red line. Salinity profiles shown at many other stations exhibit similar salinity spikes, but they are not quite as large in amplitude. In particular, the sharp vertical thermal gradient near 13.5 m at Station 2 (red line in the upper right frame of Figure A-1) caused the statistically significant salinity anomaly at that location as shown by the characteristic zigzag pattern in the green line. There was also a discharge-related reduction in salinity at Station 2, as shown in the top frame of Figure A-4, but the anomaly was shallower and was not statistically significant when compared to other salinity measurements at similar depths..

The increased salinity excursions associated with spiking were apparent in the high-resolution vertical profiles of raw temperature and salinity data that were reviewed as part of a screening analysis for salinity spikes. The figures and data presented in this report were based on CTD measurements averaged over 0.5-m depth intervals. Although not shown here, the higher-resolution profiles distinctly characterized the highly localized outliers in salinity that occurred within limited regions where there were very abrupt temperature changes. Because they were generally less than 0.5 m thick, they appear as weaker, vertically

distributed features in the lower-resolution salinity profiles included in this report (green lines in Figures A-1 through A-3).

As with salinity spikes, the erroneous transmissivity data collected in the upper water column at Station 12 overwhelm the natural and discharge-related transmissivity excursions that were present during the October 2007 survey. Their overriding influence masks the much smaller discharge-related reduction in transmissivity near the seafloor at Station 9 (top frame of Figure A-7). The Station 9 transmissivity anomaly in Table B-5 was found to be statistically significant only after the influence of the erroneous Station 12 data was removed. The importance of removing temporal drift in the DO and pH sensors is also apparent from the statistical tests on the uncorrected, raw data shown in Tables B-7 and B-8. The offsets at the beginning of the survey, when profiles at Stations 1 and 2 were being collected were large enough to generate statistically significant departures from mean conditions. The actual discharge-related pH anomaly at 7.5 m at Station 2 was highlighted only after the data were detrended (Table B-6).

Even in the absence of salinity spiking, kelp blockage, and sensor drift, the presence of statistically significant fluctuations unrelated to the discharge is expected from the nature of statistical hypothesis testing itself. From the definition of a 95% confidence level, one ‘*significant*’ departure out of every 20 measurements should occur by chance alone. With 511 measurements examined for each of the six parameters, it would not be surprising if a random few departed from the mean by an amount more than the 95% confidence interval. Moreover, when multiple hypotheses are being tested (*i.e.*, one for each observation), the error rate for each individual test should be adjusted to achieve the overall experimentwise error rate of 5% (95% confidence). By definition, this error rate is the probability that one or more of the hypothesis tests would incorrectly find a significant difference when none exists. Thus, without correcting for repeated hypothesis testing, the individual tests are conservative and “*significant*” departures will be found more often than if a single test were being performed at the experimentwise 95% confidence level.

Discharge-Related Perturbations

Despite the confounding influence of salinity spiking, kelp blockage, and sensor drift during the October 2007 survey, four distinct perturbations in seawater properties were unequivocally related to the discharge (Perturbations P1 through P4 in Table 4). A discharge-related perturbation is a group of anomalies in one or more seawater properties that are spatially contiguous at a particular station. The vertical distribution of seawater properties within and below the perturbation lends insight into which of two possible discharge processes was responsible for generating a particular anomaly.

As described previously, discharge-related anomalies are either induced by the presence of dilute wastewater constituents, or are generated by the upward displacement of ambient seawater that is entrained in the rising effluent plume. Wastewater-induced anomalies only occur when the contrast between the properties of wastewater and seawater are large enough to remain apparent after rapid initial dilution. Because of the large difference between wastewater and seawater salinity, wastewater-induced anomalies are usually only apparent in the salinity field. Under the right circumstances, however, wastewater-induced anomalies can also be apparent in density and transmissivity. Such was the case in the October 2007 survey for the measurements collected shortly after discharge (Perturbations P1 and P4 in Table 4).

Similarly, entrainment-generated anomalies are only apparent when the water column is sufficiently stratified that the juxtaposition of deep seawater properties carried upward in the rising effluent plume provides a contrast with shallow seawater properties. Upward transport of ambient seawater was

Table 4. Discharge-Related Water-Property Anomalies^a

Perturbation ^b	Station	Depth Range	Depth of Extremum	Property	Magnitude	Mechanism
P1 Dilution \geq 590:1	3	14.0 to 16.5 m	15.5 m	Salinity	-0.057 ‰	Effluent
		14.0 to 16.0 m	15.5 m	Density	-0.064 σ_t	Effluent
P2 Dilution \geq 1348:1	2	7.5 to 13.5 m	10.0 m	Salinity	-0.025 ‰	Effluent
		3.0 to 10.0 m	4.5 m	Temperature	-0.31 °C	Entrainment
		6.5 to 13.0 m	10.0 m	Transmissivity	-1.43 %	Entrainment
		6.5 to 12.5 m	7.5 m	pH	-0.021	Entrainment
P3 Dilution \geq 1348:1	1	4.0 to 12.0 m	7.0 m	Salinity	-0.025 ‰	Effluent
		6.5 to 13.0 m	9.0 m	Transmissivity	-1.41 %	Entrainment
P4 Dilution \geq 219:1	9	15.5 to 16.5 m	16.0 m	Salinity	-0.153 ‰	Effluent
		15.5 to 16.5 m	16.0 m	Density	-0.124 σ_t	Effluent
		15.5 to 16.5 m	15.5 m	Transmissivity	-2.21 %	Effluent

^a Anomalies shown in bold type were statistically significant

^b Perturbations are composed of a group of spatially coincident anomalies in several different seawater properties

responsible for generating temperature, transmissivity, and pH anomalies during the October 2007 survey (Perturbations P2 and P3 in Table 4). However, the amplitudes of these entrainment-generated anomalies were quite small compared to those measured in the last two quarterly surveys when intense upwelling conditions strongly stratified the water column and provided a large vertical contrast in seawater properties.

The mechanism that produced a discharge-related anomaly is an important consideration when assessing the discharge's compliance with the receiving-water objectives of the COP, and the requirements of the NPDES permit. As indicated in Table 4, only seven of the eleven anomalies reflected the presence of dilute wastewater, while the anomalies in other water properties were generated by entrainment of ambient seawater within the rising effluent plume. Because the thermal, transmissivity (with the exception of Station 9), and pH anomalies reflect the properties of ambient seawater that has been displaced upward, they are not subject to water-quality restrictions that were developed to limit the discharge of wastewater contaminants.

None of the salinity and density anomalies could have been generated by the movement of ambient seawater alone. For example, the top frame of Figure A-4 shows that the anomalously low salinity observed near the seafloor at Station 3 (Perturbation P1) was far lower than the ambient salinity of deep seawater at adjacent stations. Furthermore, the bottom frame of Figure A-4 shows that associated reduction in density was vertically isolated, indicating that the water-parcel with the anomalous properties was highly buoyant, and was in the process of rising farther upward into the water column. Accordingly, Perturbations P2 and P3 at Station 2 and Station 1 captured the plume's rise as it was carried northward. The rising plume was delineated by salinities of less than 33.71‰, which are shown in green and red in the top frame of Figure A-4. Salinities this low were not present in ambient seawater at depth at those two stations, so they could not have been generated by the upward displacement of naturally occurring seawater.

The transmissivity anomaly associated with Perturbation P4 was unusual because it was generated by the presence of effluent particulates. Over two decades of monitoring has shown that discharge-related anomalies in seawater properties, other than salinity and density, are almost always caused by

entrainment. However, because Perturbation P4 was measured so close to the discharge point (≥ 53 cm), it captured the plume's turbidity before it had much of a chance to dissipate within the receiving seawater. The resulting transmissivity of 74.88% was only 0.13% lower than the lowest ambient transmissivity measured just above the seafloor, within the BNL at Station 5 (Table B-5). However, given its location 1.5 m above the seafloor, the Station-9 transmissivity anomaly was clearly associated with the effluent discharge. The diffuser ports are situated on risers that extend above the seafloor diffuser structure by approximately that same height. At that height, average transmissivity at Station 9 was 2.21% higher than at the other stations. Equally important, the height of the transmissivity anomaly closely matched the density and salinity anomalies that were highly diagnostic of effluent discharge associated with Perturbation P4.

Both Perturbations P1 and P4 were measured very close to the discharge (≥ 134 cm and ≥ 53 cm). As a result, they reflected dilute effluent characteristics of the discharge that was continuing to undergo rapid dilution. The large negative density anomalies associated with these perturbations demonstrate that the effluent plume was highly buoyant at those locations, and would continue to rise swiftly through the water column. This is also apparent in the vertical density sections shown in the bottom frames of Figures A-4 and A-6. The very low-density anomalies near 16 m (delineated in green) are situated just below a layer of higher density seawater (shown in blue). Such a density inversion reflects a strong buoyancy instability that is not seen under natural conditions in the ocean because it would be rapidly dissipated during turbulent overturn. Rapid, turbulent overturn is precisely the mechanism that is expected to occur upon discharge of buoyant wastewater. This mechanism is responsible for the substantial additional dilution that occurs after the momentum of the turbulent discharge jet begins to decline. Thus, Perturbations P1 and P4 captured conditions within the turbulent jet immediately after discharge, and measured the early stages of the dilution process before buoyancy induced mixing had played a significant role in dilution.

It is noteworthy that no anomalies in DO, temperature, or pH were associated with the high-amplitude effluent-induced Perturbations P1 and P4. This supports the hypothesis that the properties of discharged wastewater contribute little to anomalies in those properties, and that discharge-related anomalies in those properties that have been observed in past surveys, and in this survey within Perturbations P2 and P3, were generated instead by the upward displacement of ambient seawater. Except for salinity, the contrast between seawater and wastewater properties is so minimal that they rapidly disappear with even a small amount of dilution.

Thus, anomalies in these other water properties are largely determined by the degree of water column stratification. In particular, during the October 2007 survey, the DO field was nearly uniform with a total range of only 0.9 mg/L. Consequently, in the absence of strong vertical differences in DO, entrainment-generated anomalies were not readily apparent in that water property, although an upward extension of seawater with slightly lower DO is barely discernable at Station 2 (delineated in green in the middle frame of Figure A-5). In contrast, the small entrainment-generated anomalies in temperature, transmissivity, and pH at Station 2 are much more apparent. Because of how they are generated, these anomalies tend to cover a broad vertical extent as opposed to the effluent induced anomalies, which tend to be highly localized. For example, the upward bowing of isotherms at Station 2 (middle frame of Figure A-4) is apparent at all depth levels between 3 m and 13.5 m. This, along with the distribution of salinity at Stations 1 and 2 (shown in the top frame of Figure A-4), demonstrates that the plume did not become trapped at depth below a thermocline, and instead, had achieved maximum dilution during its turbulent rise to the sea surface. This contrasts with modeling conducted to determine the critical initial dilution which assumes the water column is heavily stratified, and dilution is limited by a plume that becomes

trapped below the sea surface. This was not the case for the October 2007 survey, and as described below, the ultimate dilution achieved by the discharge far exceeded the dilution predicted by modeling.

Initial Dilution Computations

The amplitude of the negative salinity anomalies at Stations 1, 2, 3, and 9 lends insight into the effectiveness of the outfall at dispersing effluent and, ultimately, compliance with the receiving-water objectives of the COP and NPDES discharge permit. The critical initial dilution applicable to the MBCSD outfall was conservatively estimated to be 133:1 (Tetra Tech 1992). This estimate was based on worst-case modeling under highly stratified conditions where the trapping of the plume below the thermocline limited the mixing achieved during the buoyant plume's rise through the water column. The dispersion modeling determined that, after initial mixing was complete, 133 parts of ambient water would have mixed with each part of wastewater. The modeling predicted that this dilution would be achieved after the plume rose only 9 m from the seafloor, whereupon it would become trapped beneath a thermocline and spread laterally with no further substantive dilution. A 9-m rise translates into a trapping depth that is 6.4 m below the sea surface.

However, as described below, computations of dilution based on the salinity anomalies measured near the seafloor shortly after discharge demonstrate that the effluent plume actually achieved a far higher dilution ($\geq 219:1$) than the total dilution (133:1) predicted by conservative modeling. Thus, rapid mixing associated with the momentum of the discharge jet alone is capable of achieving all of the dilution predicted by modeling, without even considering the additional dilution that is provided by the buoyant rise of the plume over a distance of 9 m. This demonstrates that the diffuser structure was operating far more efficiently than predicted by the modeling.

The conservative nature of the dilution ratio determined from modeling is an important consideration because it was used to specify permit limitations on chemical concentrations in wastewater discharged from the treatment plant. These end-of-pipe effluent limitations were back-calculated from the receiving-water objectives listed in the COP (SWRCB 1997) using the 133:1 dilution ratio determined from the modeling. Use of a higher critical dilution ratio would relax the stringent end-of-pipe effluent limitations that were thought to be necessary in order to meet Ocean-Plan standards.

End-of-pipe limitations on contaminant concentrations within effluent were based on the definition of dilution (Fischer et al. 1979). From the mass-balance of a conservative tracer, the concentration of a particular contaminant within effluent before discharge (C_e) can be determined from Equation 1.

$$C_e \equiv C_o + D (C_o - C_s) \quad \text{Equation 1}$$

where: C_e = the concentration of a constituent in the effluent,
 C_o = the concentration of the constituent in the ocean after dilution by D (*i.e.*, the COP objective),
 D = the dilution ratio of the volume of seawater mixed with effluent, and
 C_s = the background concentration of the constituent in ambient seawater.

By rearranging Equation 1, the actual dilution achieved by the outfall can also be determined from measured seawater anomalies. This measured dilution can then be compared with the critical dilution factor determined from modeling. Salinity is an especially useful tracer because it directly reflects the magnitude of ongoing dilution. Specifically, the salinity concentration in effluent is negligible so C_e is eliminated in Equation 1 and the dilution ratio (D) can be computed from the salinity anomaly ($A = C_o - C_s$) as:

$$D = \frac{-C_o}{(C_o - C_s)} \equiv \frac{-C_o}{A} \quad \text{Equation 2}$$

where: D = the dilution ratio of the volume of seawater mixed with effluent,
 C_o = the salinity of the effluent-seawater mixture after dilution by D ,
 C_s = the background seawater salinity (approximately 32.9‰), and
 $A = C_o - C_s$ = the salinity anomaly.

The magnitudes of the observed salinity anomalies were used in Equation 2 to compute the actual dilution levels associated with each of the four Perturbations. These computed dilutions are listed in the left column of Table 4. As expected, Perturbation P4, which was measured closest to the diffuser structure, had the largest-amplitude salinity anomaly (-0.153%), and lowest dilution (219:1). Perturbation P4 was located only 53 cm from the diffuser structure. Diffuser ports are situated every 1.5 m along diffuser structure, so Perturbation P4 was at most only 1.3 m from a port, and well within the turbulent ejection jet emanating from that port. Perturbation P1 was measured slightly farther (134 cm) from the diffuser structure and, accordingly, had a smaller-amplitude salinity anomaly (-0.057%) resulting from the additional dilution achieved with greater distance. Finally, after additional mixing during a buoyant rise of only 5 m (Perturbation P2), the salinity signature was almost imperceptible (-0.025%) owing to a dilution of more than 1000-fold.

Given its greater depth, the dilution level within Perturbation P2 should theoretically be lower than the model predictions because the effluent plume had not experienced as much buoyancy induced dispersion as predicted by modeling at 6.4 m below the sea surface. Instead, the actual dilution achieved at that point was ten-times larger than the dilution predicted by conservative modeling. These dilution computations demonstrate that, during the October 2007 survey, the outfall was performing far better than designed, and was rapidly diluting effluent more than 219-fold within as little as 53 cm of the discharge point. Consequently, COP receiving-water objectives were being easily met by the chemical concentration limits promulgated by the NPDES discharge permit issued to the MBCSD.

DISCUSSION

Sampling during the October 2007 survey demonstrated that the wastewater discharge was in compliance with the receiving-water limitations specified in the NPDES permit, and with the water-quality objectives of the COP (SWRCB 1997) and the Central Coast Basin Plan (RWQCB 1994). Specifically, there were no particulates of sewage origin seen floating on the ocean surface at any of the stations sampled during the October 2007 water-quality survey, and the discharge complied with all quantitative limits on seawater properties.

Although discharge-related changes in five of the six water properties were observed during the October 2007 survey, the changes were either not statistically significant, were measured very close to a diffuser port and well within the boundary of the ZID before initial dilution was complete, or resulted from the displacement of ambient seawater rather than the presence of effluent constituents. Receiving-water limitations only apply to statistically significant changes caused by the presence of effluent constituents beyond the ZID boundary. Regardless, the measurements collected during the October 2007 survey demonstrated that the receiving-water limitations were being met within less than a few meters of the discharge. Beyond the ZID, at Stations 1 and 2 (Perturbations P2 and P3), the effluent had experienced such a high level of dilution that no perceptible changes in seawater properties were caused by the presence of effluent constituents, except a very slight reduction in salinity. The discharge-related anomalies in temperature, transmissivity, and pH recorded during the survey were all generated by the upward displacement of ambient seawater, and not the presence of dilute effluent. This is an important consideration because seawater limitations promulgated in the COP restrict attention to changes caused by the presence of waste materials, not the movement of ambient seawater.

Outfall Performance

The large salinity anomalies measured in the turbulent ejection jets close to a diffuser port demonstrated that the receiving-water objectives of the COP were being met at depth, well within the ZID. These high-precision observations demonstrated that the turbulent jet was achieving dilutions exceeding the minimum critical dilution of 133:1 within 1.3 m of a discharge port. The amplitude of the greatest salinity anomaly indicates that wastewater had been diluted more than 219-fold at this location. Thus, the dilution objective was achieved without consideration of the substantial additional dilution provided by the buoyant plume's subsequent rise through the water column. The high dilution ratio that was determined from actual measurements during the October 2007 survey demonstrated that the outfall was performing better than expected, and that the limits on wastewater contaminant concentrations specified in the MBCSD NPDES discharge permit would easily meet the receiving-water objectives of the California Ocean Plan (COP).

NPDES Permit Limits

The seawater properties measured during the October 2007 survey were statistically evaluated for compliance with the pertinent receiving-water limitations promulgated by the NPDES discharge permit and the COP. Specifically, the permit and COP state that the discharge shall not cause the occurrence of the following conditions.

1. *Natural light to be significantly reduced at any point outside the initial dilution zone as the result of the discharge of waste*

2. *The dissolved oxygen concentration outside the zone of initial dilution to fall below 5.0 mg/L or to be depressed more than 10 percent from that which occurs naturally*
3. *The pH outside the zone of initial dilution to be depressed below 7.0, raised above 8.3, or changed more than 0.2 units from that which occurs naturally*
4. *Temperature of the receiving water to adversely affect beneficial uses*

The COP (SWRCB 1997) further defines a ‘*significant*’ difference as ‘*...a statistically significant difference in the means of two distributions of sampling results at the 95 percent confidence level.*’ For each observation in Tables B-1 through B-8, the statistical significance of departures from mean conditions at a given depth level were determined with an analysis of variance that compared a single observation with the mean of a larger set of samples (Sokal and Rohlf 1997, p228; Ury 1976). Although 15 independent hypothesis tests were performed at each depth level, no Bonferroni adjustment to the error rate was included, so the tests are conservative. Specifically, Bonferroni adjustment indicates that the actual confidence level for the overall null hypothesis test for differences in properties is higher, around 99.7%, rather than the 95% level that applies to a single test. The standard deviation that was applied in the tests was determined from the entire data set to reflect the full range in ambient properties, including vertical variations.

Light Transmittance

Statistical analysis revealed significant changes in instrumentally recorded light transmittance at two of the sixteen monitoring stations during in the October 2007 survey (highlighted by bold typeface in Table B-5). Although statistically significant, the anomalies at Station 12 were generated by the entanglement of what was likely a piece of detached kelp that intermittently blocked the light path of the transmissometer. The data recorded at Station 12 was therefore an artifact of sampling and was not associated with the diffuser structure or wastewater plume.

Table B-5 shows one significant reduction in transmissivity near the seafloor at Station 9. However, Station 9 lies within the ZID where the COP limitation does not apply. Furthermore, the transmissivity anomaly was observed at depth, where little natural light penetrates. The transmissivity anomaly was located at 15.5 m, which was close to the deepest boundary of the 16-m euphotic zone (twice the maximum Secchi depth of 8.0 m listed in Table B-9). Thus, at that location, the presence of this “*significant*” transmissivity anomaly could not have caused a significant “*...reduction in the transmittance of natural light...*” The other two discharge-related transmissivity anomalies were not statistically significant, and were not generated “*...as the result of the discharge of waste*” (SWRCB 1997). Instead, the turbidity anomalies in the mid-water column associated with Perturbations P2 and P3 were generated by the upward movement of ambient seawater, not the presence of wastewater particulates.

Dissolved Oxygen

Although it is not explicitly stated in the NPDES discharge permit, the COP specifies that the DO limitation only applies to reductions that occur “*...as a result of the discharge of oxygen demanding waste materials.*” However, effluent samples routinely collected prior to discharge demonstrate that the treatment process is highly effective at removing oxygen demanding material from the wastestream. As a result, reductions in DO caused by effluent constituents have never been observed within the receiving waters. Accordingly, during the October 2007 survey, none of the DO measurements were found to depart from mean conditions by more than the 95% confidence interval (Table B-4). In addition, no DO

deviations were found to spatially coincide with discharge-related anomalies in other seawater properties. Spatial coincidence would suggest that they were related to the discharge. Regardless of their lack of statistical significance or relationship to the discharge, all 511 of the DO measurements collected during the October 2007 survey complied with the numerical limits on DO deviations in the discharge permit. All of the DO measurements remained between 6.04 and 6.92 and thus were well above the 5-mg/L minimum specified in the Basin Plan and the NPDES discharge permit. Consequently, no DO measurements were found to be statistically significant, and therefore, would not be considered “...depressed more than 10 percent from that which occurs naturally.”

pH

The only statistically significant lateral anomaly in pH (Table B-6) was measured at mid-depth at Station 2. As with the other water properties, this pH anomaly was generated by the upward displacement of ambient bottom water, which is naturally low in pH. Moreover, the maximum amplitude of this anomaly (-0.021) was so small that it easily complied with the numerical limit that restricts changes to less than 0.2 pH units. In fact, the range in pH among all of the measurements was only 0.047, so none of the measurements can be considered changed by ‘...more than 0.2 pH units from that which occurs naturally.’ The range across the entire pH field remained between 8.19 and 8.24, and thus, all of the measurements also complied with the lower (7.0 pH) and upper (8.3 pH) bounds on discharge-induced pH changes.

Temperature and Salinity

The total range in temperature of 0.88°C across all observations was largely due to naturally occurring vertical stratification. Even if changes this large were generated by the discharge, they would be considered too small ‘...to adversely affect beneficial uses....’ The observed temperature range was much less than the large-scale spatial variability in sea-surface temperature shown in the satellite image on the cover of this report. The small, discharge-induced decreases in temperature (-0.31°C) that were visually apparent in the vertical section at Station 2 clearly resulted from the upward displacement of naturally occurring, cooler bottom water rather than as a result of the presence of warmer wastewater constituents. In any regard, the slightly depressed mid-depth temperature was comparable to average temperatures measured near the seafloor throughout the October 2007 survey. Accordingly, the Station 2 thermal anomaly was not found to be statistically significant.

Additionally, although salinity anomalies provide the best tracer of discharged effluent, their actual maximum amplitude (-0.153‰) during the October 2007 survey was small compared to the seasonal and spatial differences in salinity that occur along the south-central California coast. For example, seasonal differences in average salinity at this location are four times higher (0.64‰) than the largest salinity anomaly recorded during the October 2007 survey. In any regard, the observed ranges in both the reported temperature (0.88°C) and salinity (-0.180‰) across all data collected during the October 2007 survey were too small to be considered harmful to marine biota or deleterious to beneficial uses.

Conclusions

All of the measurements recorded during the October 2007 survey complied with the receiving-water limitations specified in the NPDES discharge permit. The discharge-related anomalies that were found just above the seafloor at Stations 3 and 9 were caused by the presence of dilute effluent located within a centimeters to just a few meters of a discharge port. Salinity measurements demonstrated that wastewater

was undergoing rapid mixing of more than 200-fold within only a few feet of discharge from the diffuser structure. Additionally, the dilution levels achieved by the momentum of the jet alone immediately after discharge were over one-and-a-half times larger than those predicted by modeling for the entire dilution process. Measurements within the effluent plume recorded at mid-depth beyond the ZID demonstrated a dilution of more than 1300-fold had been achieved. These measurements confirmed that the diffuser structure and the outfall were operating better than would be expected from the modeling.

REFERENCES

- California Department of Fish and Game (CDFG). 2000. Black Rockfish, *Sebastes melanops*, 1993-1999 Commercial Catch by Ports & Blocks. In: Volume 1, Marine Fisheries Profiles. California Department of Fish and Game, Marine Region. December 2000.
- Davis, R.E., J.E. Dufour, G.J. Parks, and M.R. Perkins. 1982. Two Inexpensive Current-Following Drifters. Scripps Institution of Oceanography, University of California, San Diego, La Jolla, California. SIO Reference No. 82-28. December 1982.
- Dohl, T.D., R.C. Guess, M.L. Duman, R.C. Helm. 1983. Cetaceans of central and northern California, 1980-1983: status, abundance, and distribution. Prepared for the U.S. the Department of the Interior, Minerals Management Service, Pacific OCS Region, Los Angeles, California. pp. 284.
- Fischer, H.B., E.J. List, R.C.Y. Koh, J. Imberger, and N.H. Brooks. 1979. Mixing in Inland and Coastal Waters. New York: Academic Press, 483 p.
- Herzing, D.L. and B.R. Mate. 1984. Gray whale migration along the Oregon coast, 1978-1981. In: M.L. Jones, S.L. Swartz, and S. Leatherwood [Eds.]. The Gray Whale, *Eschrichtius robustus*. Academic Press: Orlando, Florida. pp. 289-307.
- Kuehl, S.A., C.A. Nittrouer, M.A. Allison, L. Ercilio, C. Faria, D.A. Dukat, J.M. Jaeger, T.D. Pacioni, A.G. Figueiredo, and E.C. Underkoffler 1996. Sediment deposition, accumulation, and seabed dynamics in an energetic fine-grained coastal environment. *Continental Shelf Research*, 16: 787-816.
- Marine Research Specialists (MRS). 1998a. City of Morro Bay and Cayucos Sanitary District, Offshore Monitoring and Reporting Program, Water Column Sampling, March 1998 Survey. Prepared for the City of Morro Bay, CA. April 1998.
- Marine Research Specialists (MRS). 1998b. City of Morro Bay and Cayucos Sanitary District, Offshore Monitoring and Reporting Program, Semiannual Benthic Sampling Report, April 1998 Survey. Prepared for the City of Morro Bay, CA. July 1998.
- Marine Research Specialists (MRS). 1998c. City of Morro Bay and Cayucos Sanitary District, Offshore Monitoring and Reporting Program, Water Column Sampling, July 1998 Survey. Prepared for the City of Morro Bay, CA. August 1998.

- Marine Research Specialists (MRS). 2000. City of Morro Bay and Cayucos Sanitary District, Offshore Monitoring and Reporting Program, 1999 Annual Report. Prepared for the City of Morro Bay, California. February 2000.
- Marine Research Specialists (MRS). 2001. City of Morro Bay and Cayucos Sanitary District, Offshore Monitoring and Reporting Program, 2000 Annual Report. Prepared for the City of Morro Bay, California. February 2001.
- Marine Research Specialists (MRS). 2002. City of Morro Bay and Cayucos Sanitary District, Offshore Monitoring and Reporting Program, 2001 Annual Report. Prepared for the City of Morro Bay, California. February 2002.
- Marine Research Specialists (MRS). 2003. City of Morro Bay and Cayucos Sanitary District, Offshore Monitoring and Reporting Program, 2002 Annual Report. Prepared for the City of Morro Bay, California. February 2003.
- Marine Research Specialists (MRS). 2004. City of Morro Bay and Cayucos Sanitary District, Offshore Monitoring and Reporting Program, 2003 Annual Report. Prepared for the City of Morro Bay, California. February 2004.
- Marine Research Specialists (MRS). 2005. City of Morro Bay and Cayucos Sanitary District, Offshore Monitoring and Reporting Program, 2004 Annual Report. Prepared for the City of Morro Bay, California. February 2005.
- Marine Research Specialists (MRS). 2006. City of Morro Bay and Cayucos Sanitary District, Offshore Monitoring and Reporting Program, 2005 Annual Report. Prepared for the City of Morro Bay, California. February 2006.
- Marine Research Specialists (MRS). 2007. City of Morro Bay and Cayucos Sanitary District, Offshore Monitoring and Reporting Program, 2006 Annual Report. Prepared for the City of Morro Bay, California. February 2007.
- Morro Group, Inc. 2000. MFS Globenet Corp./WorldCom Network Services Fiber Optic Cable Project Final Environmental Impact Report. SCH No. 98091053. Volume I. Submitted to: County of San Luis Obispo Department of Planning and Building. Prepared in association with Arthur D. Little, Inc. and Marine Research Specialists. January 2000.
- Regional Water Quality Control Board (RWQCB) - Central Coast Region. 1994. Water Quality Control Plan (Basin Plan) Central Coast Region. Available from the RWQCB at 81 Higuera Street, Suite 200, San Luis Obispo, California. 148p. + Appendices.
- Regional Water Quality Control Board (RWQCB) - Central Coast Region. 1998. Administrative Extension of Waste Discharge Requirements/National Pollution Discharge Elimination System (NPDES) CA0047881, Order 92-67. Letter to Mr. William Boucher, Director of Public Works, City of Morro Bay from Roger W. Briggs, Executive Officer. 10 April 1998.

- Regional Water Quality Control Board (RWQCB) - Central Coast Region and the Environmental Protection Agency (EPA) – Region IX. 1998a. Waste Discharge Requirements (Order No. 98-15) and National Pollutant Discharge Elimination System (Permit No. CA0047881) for City of Morro Bay and Cayucos Sanitary District, San Luis Obispo County. 11 December 1998.
- Regional Water Quality Control Board (RWQCB) - Central Coast Region and the Environmental Protection Agency (EPA) – Region IX. 1998b. Monitoring and Reporting Program No. 98-15 for City of Morro Bay and Cayucos Sanitary District, San Luis Obispo County. 11 December 1998.
- Reilly, S.B. 1984. Assessing gray whale abundance: a review. In: M.L. Jones, S.L. Swartz, and S. Leatherwood [Eds.]. *The Gray Whale, Eschrichtius robustus*. Orlando, Florida: Academic Press. pp. 203-223.
- Rice, D.W., A.A. Wolman and H.W. Braham. 1984. The gray whale, *Eschrichtius robustus*. In: J.M. Briewick and H.W. Braham [Eds.]. *The Status of Endangered Whales*. Mar. Fish. Rev. 46(4):7-14.
- Rugh, D.J. 1984. Census of gray whales at Unimak Pass, Alaska: November-December 1977-1979. In: M.L. Jones, S.L. Swartz, and S. Leatherwood. (Eds.). *The Gray Whale, Eschrichtius robustus*. Orlando, Florida: Academic Press. pp. 225-248.
- Sea-Bird Electronics, Inc. (SBE) 1989. Calculation of M and B Coefficients for the Sea-Tech Transmissometer. Application Note No. 7, Revised September 1989.
- Sea-Bird Electronics, Inc. (SBE) 1993. SBE 13/22/23/30 Dissolved Oxygen Sensor Calibration and Deployment. Application Note No. 13-1, rev B, Revised April 1993.
- Sokal, R.R. and F.J. Rohlf. 1997. *Biometry: the Principals and Practice of Statistics in Biological Research*, 3rd ed. New York: W.H. Freeman and Company, 850 p.
- Southern California Bight Pilot Project Field Coordination Team (SCBPPFCT). 1995. *Field Operation Manual for Marine Water-Column, Benthic, and Trawl monitoring in Southern California*. August 22, 1995.
- State Water Resources Control Board (SWRCB). 1997. *Water quality control plan, ocean waters of California, California Ocean Plan*. California Environmental Protection Agency. Effective July 23, 1997.
- Sund, P.N. and J.L. O'Connor. 1974. Aerial observations of gray whales during 1973. Mar. Fish. Rev. 36(4):51-55.
- Tetra Tech. 1992. *Technical Review City of Morro Bay, CA Section 301(h) Application for Modification of Secondary Treatment Requirements for a Discharge into Marine Waters*. Prepared for the U.S. Environmental Protection Agency, Region IX, San Francisco, CA by Tetra Tech, Inc., Lafayette, CA. February 1992.
- Ury, H.K. 1976. A comparison of four procedures for multiple comparisons among means (pairwise contrasts) for arbitrary sample sizes. *Technometrics*, 18: 89–97.

APPENDIX A

Water Quality Profiles and Cross Sections

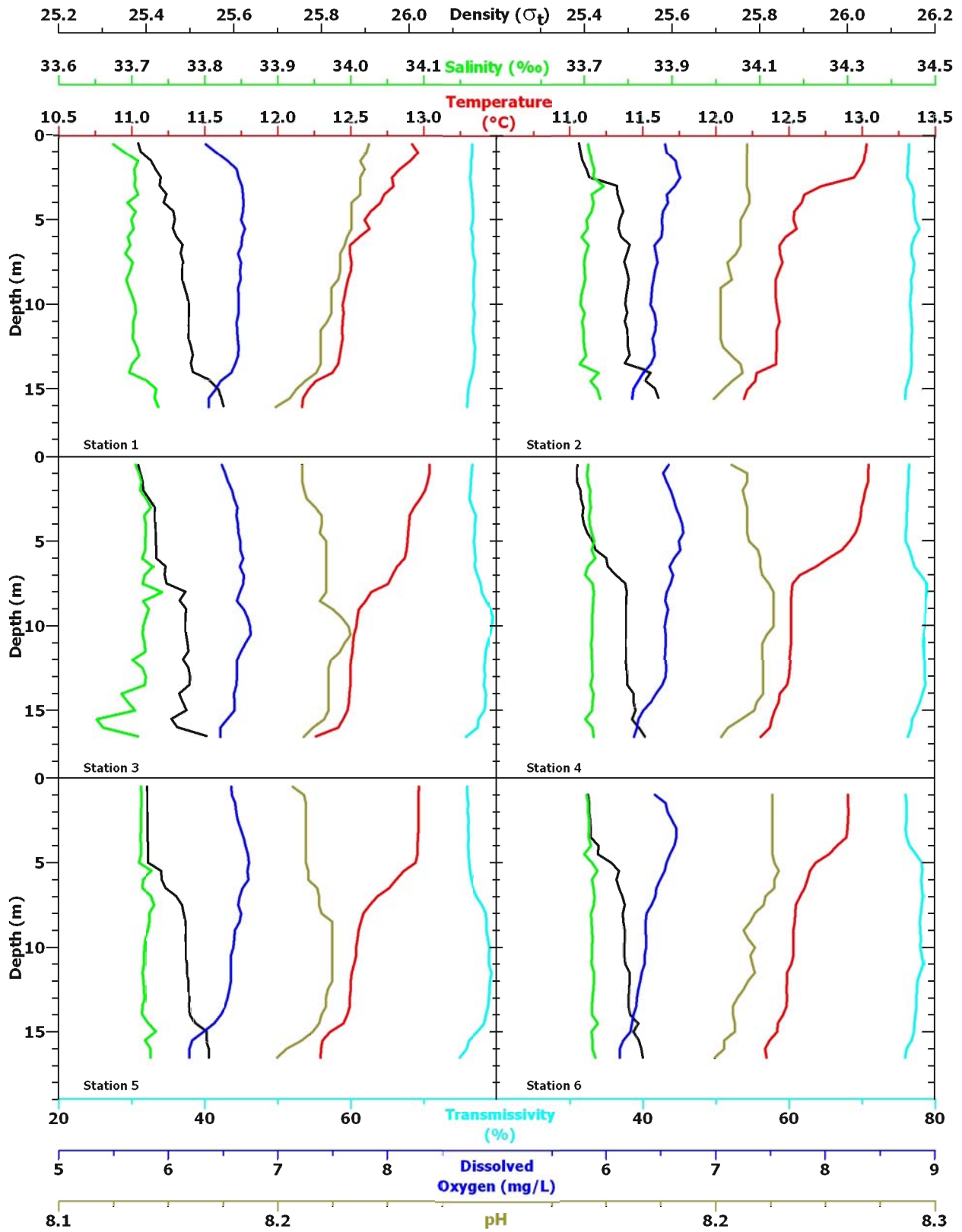


Figure A-1. Vertical Profiles of Water-Quality Parameters for Stations 1 through 6 measured on 9 October 2007

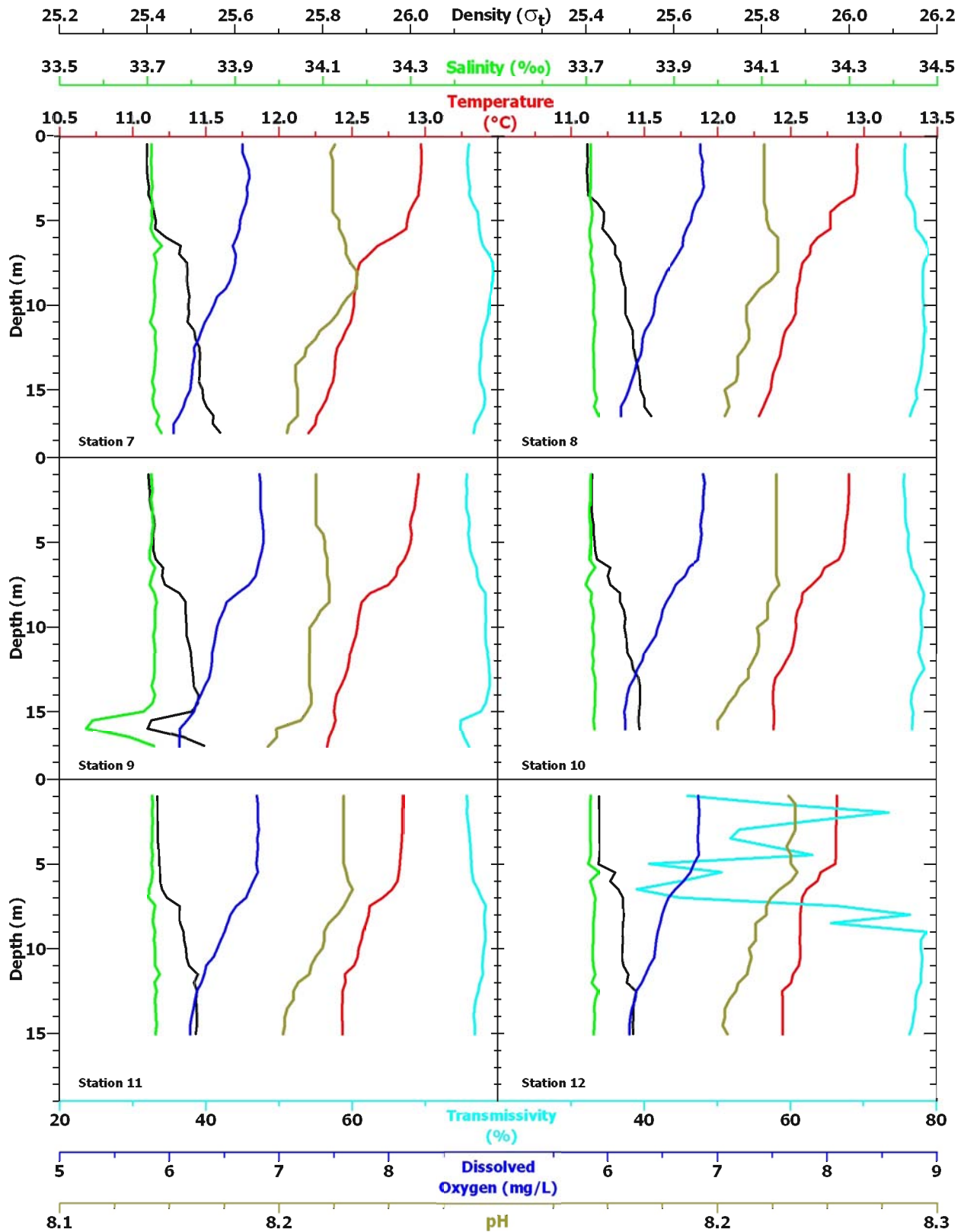


Figure A-2. Vertical Profiles of Water-Quality Parameters for Stations 7 through 12 measured on 9 October 2007

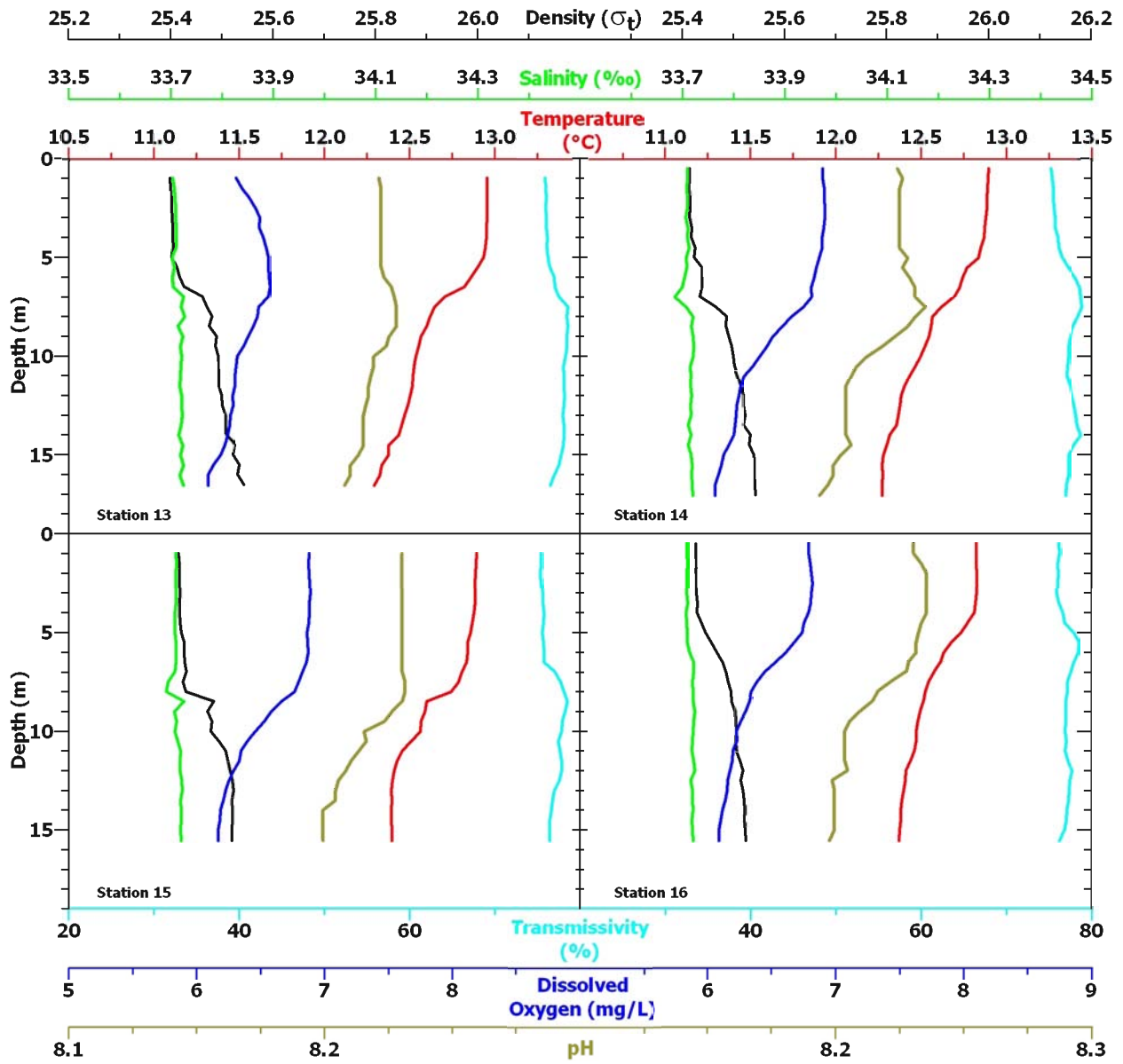


Figure A-3. Vertical Profiles of Water-Quality Parameters for Stations 13 through 16 measured on 9 October 2007

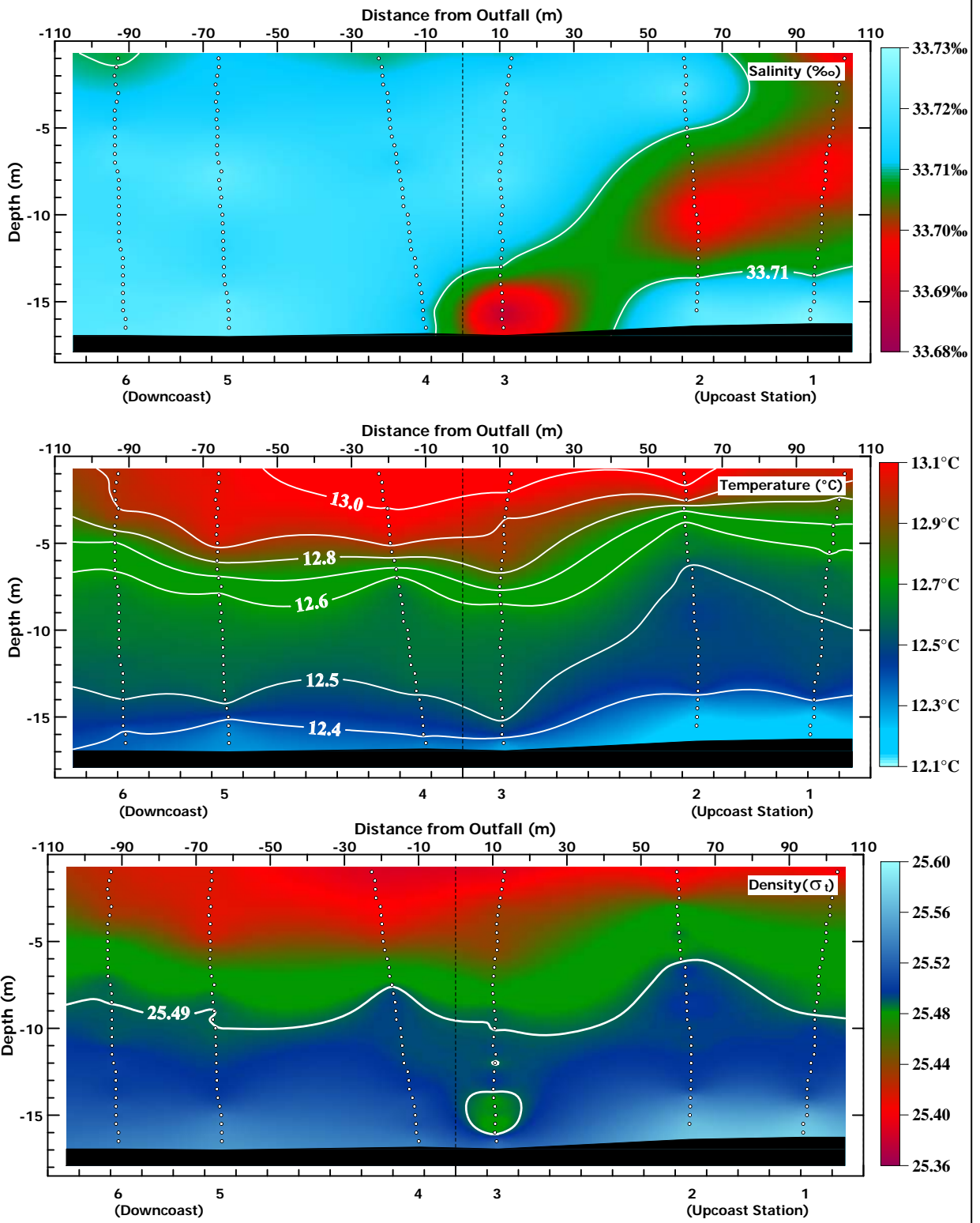


Figure A-4. Along-Shore Transects of Salinity, Temperature, and Density on 9 October 2007

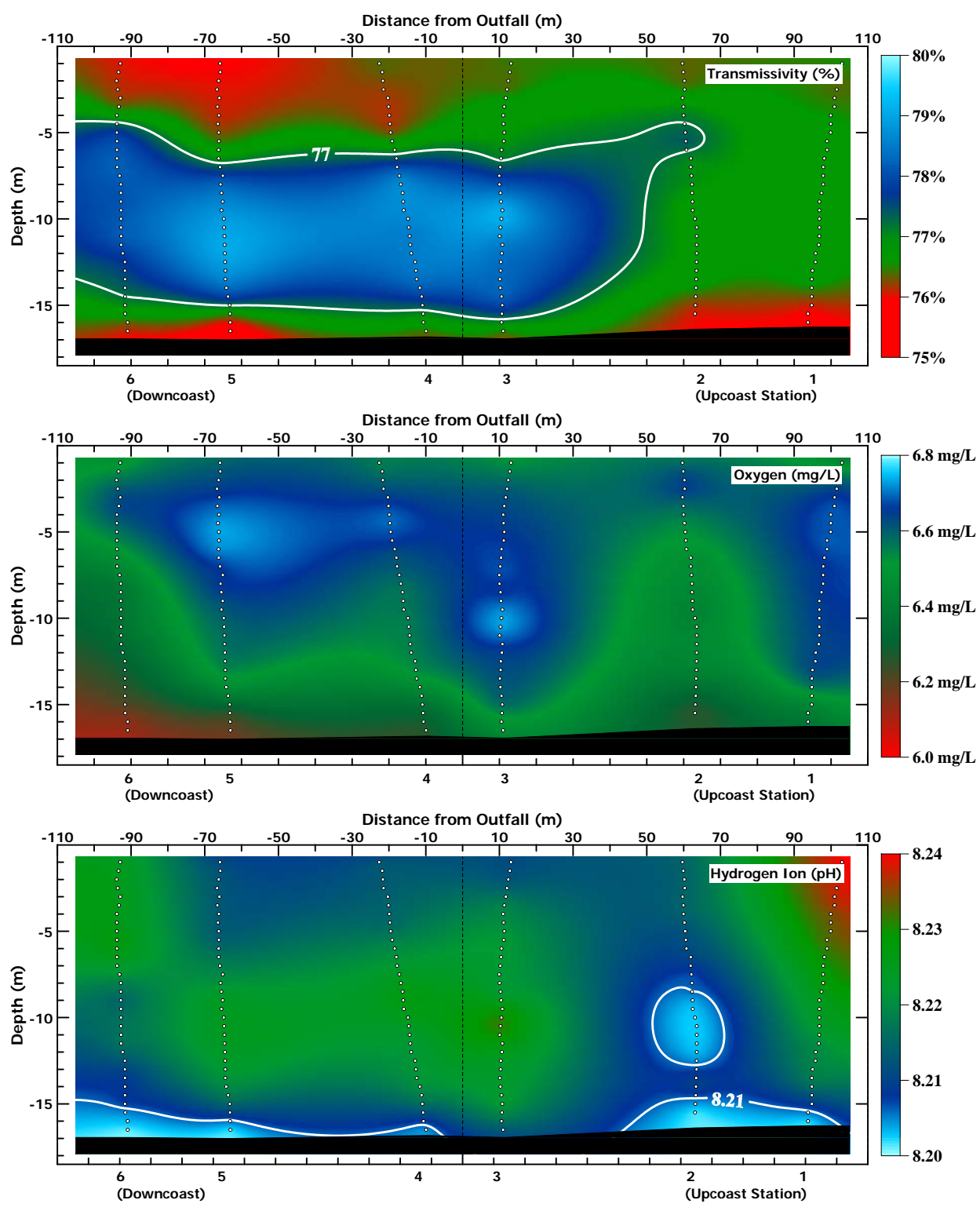


Figure A-5. Along-Shore Transects of Transmissivity, Oxygen, and pH on 9 October 2007

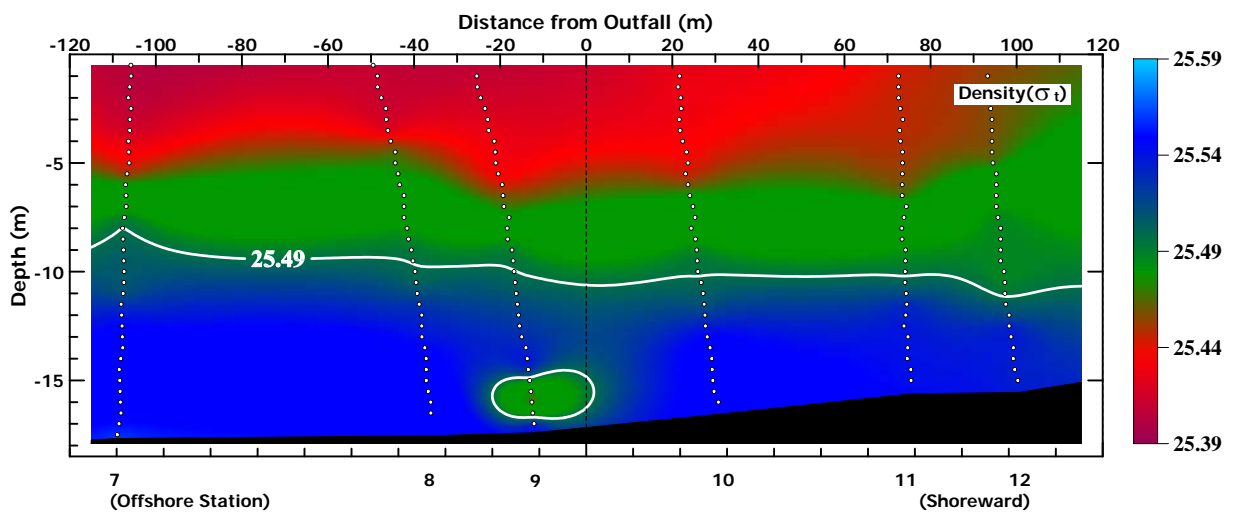
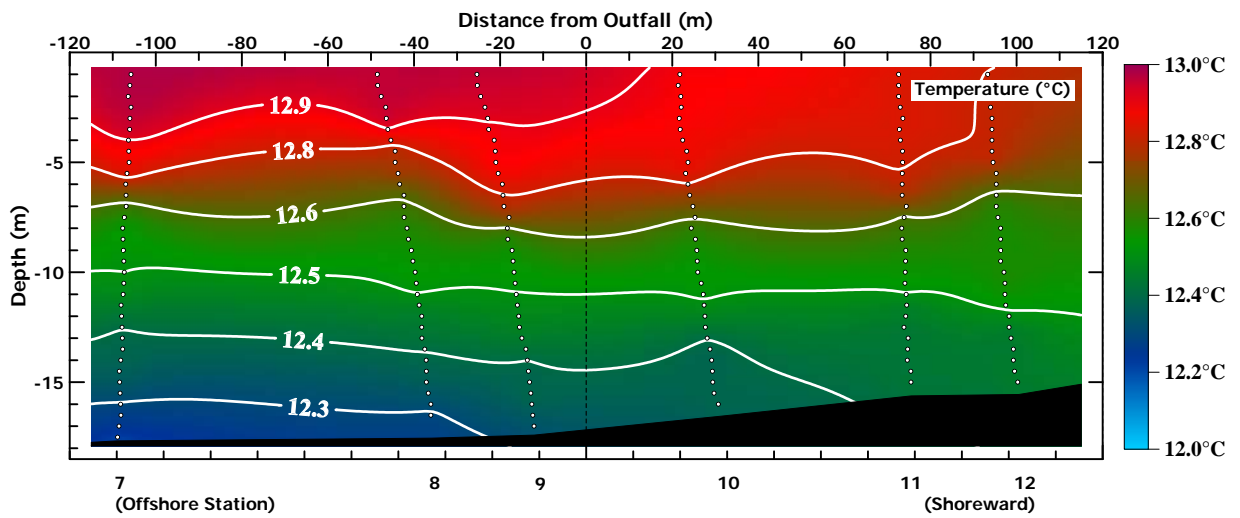
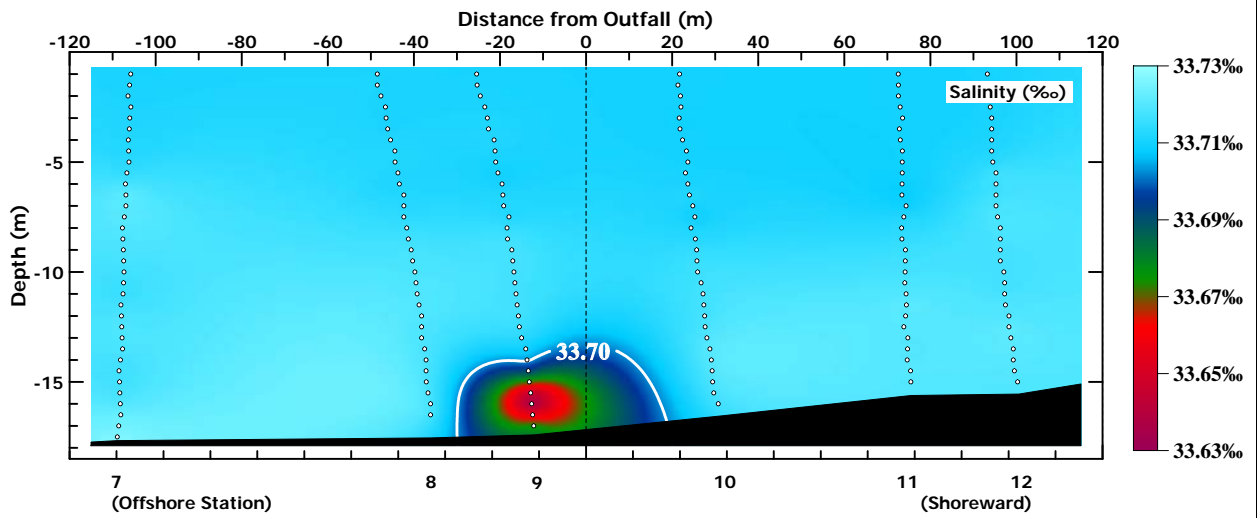


Figure A-6. Cross-Shore Transects of Salinity, Temperature, and Density on 9 October 2007

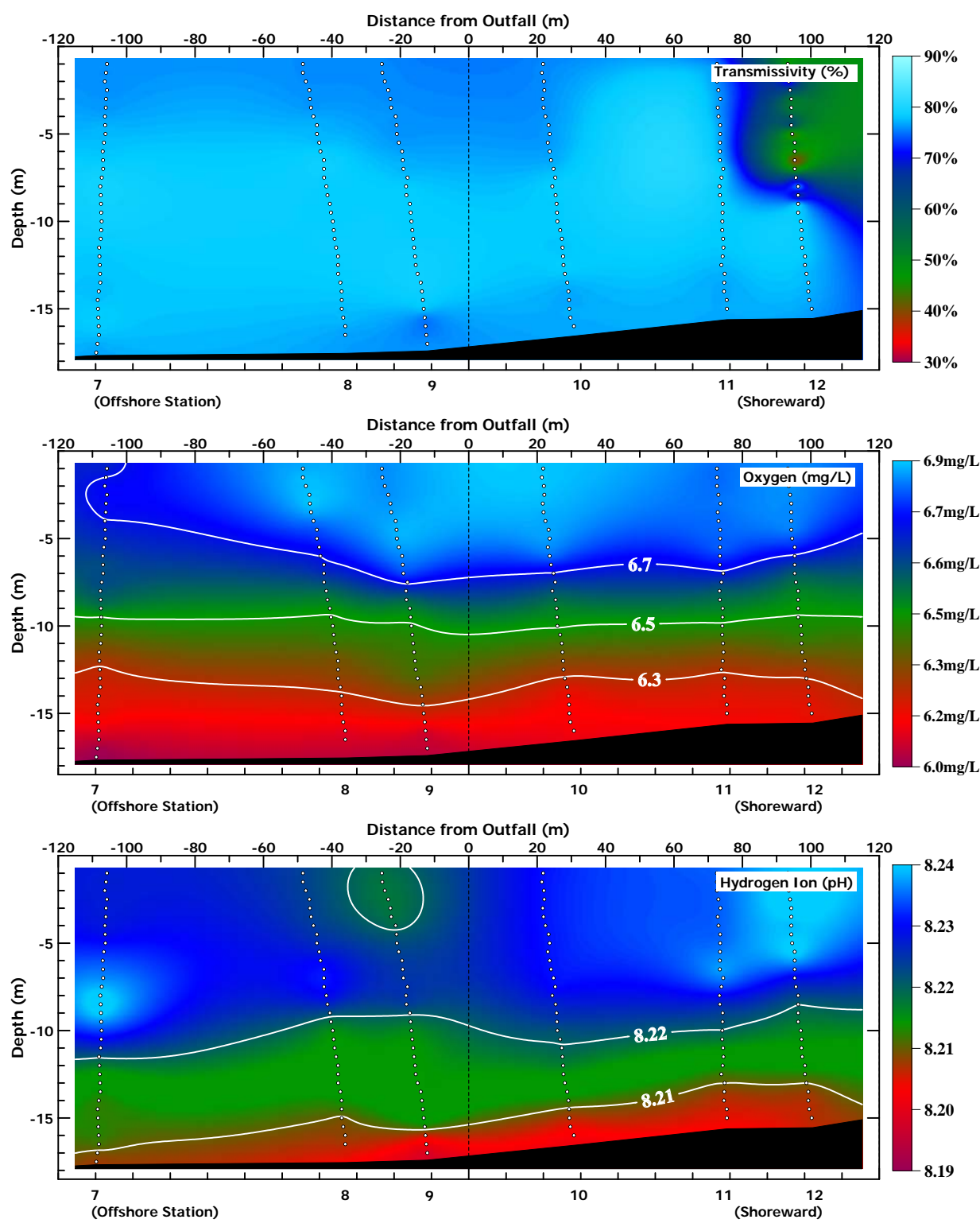


Figure A-7. Cross-Shore Transects of Transmissivity, Oxygen, and pH on 9 October 2007

APPENDIX B

Tables of Profile Data and Standard Observations

Table B-2. Salinity¹ on 9 October 2007

Depth (m)	Salinity (‰)															
	1	2	3	4	5	6	7	8	9	10	11	12	13	14	15	16
0.5	33.675	33.709	33.705	33.709	33.713		33.711	33.711						33.710		33.709
1.0	33.691	33.713	33.710	33.707	33.713	33.706	33.711	33.711	33.710	33.711	33.709	33.711	33.704	33.710	33.711	33.709
1.5	33.708	33.715	33.713	33.708	33.713	33.709	33.710	33.711	33.711	33.710	33.710	33.710	33.707	33.709	33.712	33.710
2.0	33.703	33.721	33.711	33.713	33.713	33.709	33.711	33.711	33.712	33.710	33.710	33.710	33.709	33.710	33.711	33.709
2.5	33.705	33.720	33.719	33.712	33.713	33.711	33.711	33.711	33.708	33.710	33.710	33.710	33.709	33.710	33.711	33.709
3.0	33.704	33.742	33.725	33.714	33.712	33.712	33.713	33.711	33.712	33.708	33.710	33.710	33.709	33.706	33.711	33.709
3.5	33.709	33.716	33.716	33.711	33.712	33.710	33.709	33.709	33.712	33.708	33.709	33.710	33.711	33.711	33.710	33.711
4.0	33.694	33.720	33.719	33.713	33.712	33.716	33.713	33.712	33.714	33.710	33.709	33.711	33.710	33.710	33.708	33.708
4.5	33.705	33.716	33.718	33.717	33.713	33.700	33.710	33.714	33.711	33.710	33.710	33.711	33.710	33.713	33.708	33.709
5.0	33.699	33.705	33.718	33.722	33.710	33.717	33.712	33.713	33.711	33.711	33.709	33.706	33.703	33.708	33.709	33.710
5.5	33.702	33.707	33.718	33.717	33.727	33.730	33.708	33.709	33.706	33.709	33.710	33.730	33.708	33.709	33.711	33.710
6.0	33.695	33.694	33.714	33.724	33.715	33.718	33.717	33.709	33.707	33.707	33.708	33.710	33.704	33.704	33.711	33.714
6.5	33.698	33.709	33.728	33.707	33.715	33.721	33.734	33.713	33.717	33.721	33.703	33.716	33.705	33.700	33.711	33.722
7.0	33.691	33.702	33.717	33.702	33.727	33.724	33.716	33.710	33.711	33.708	33.703	33.721	33.724	33.686	33.709	33.722
7.5	33.701	33.699	33.714	33.719	33.731	33.722	33.722	33.715	33.706	33.700	33.717	33.720	33.719	33.708	33.695	33.720
8.0	33.698	33.700	33.741	33.722	33.724	33.715	33.720	33.713	33.717	33.713	33.714	33.719	33.727	33.721	33.691	33.721
8.5	33.693	33.701	33.715	33.720	33.724	33.717	33.717	33.717	33.721	33.712	33.713	33.717	33.715	33.718	33.726	33.721
9.0	33.696	33.697	33.723	33.719	33.723	33.718	33.718	33.719	33.718	33.717	33.718	33.716	33.723	33.721	33.707	33.724
9.5	33.701	33.692	33.718	33.718	33.718	33.719	33.719	33.718	33.717	33.717	33.715	33.717	33.718	33.723	33.712	33.722
10.0	33.704	33.691	33.715	33.717	33.717	33.718	33.716	33.718	33.717	33.715	33.718	33.716	33.720	33.721	33.709	33.722
10.5	33.705	33.700	33.715	33.717	33.716	33.717	33.715	33.717	33.714	33.718	33.717	33.715	33.720	33.716	33.715	33.720
11.0	33.702	33.695	33.717	33.716	33.717	33.716	33.708	33.721	33.716	33.718	33.718	33.716	33.719	33.717	33.720	33.719
11.5	33.702	33.697	33.718	33.716	33.714	33.722	33.719	33.720	33.717	33.714	33.727	33.721	33.718	33.717	33.718	33.723
12.0	33.701	33.698	33.701	33.716	33.716	33.722	33.718	33.718	33.717	33.718	33.717	33.713	33.720	33.719	33.719	33.724
12.5	33.707	33.699	33.715	33.716	33.716	33.721	33.721	33.717	33.717	33.716	33.721	33.727	33.720	33.717	33.722	33.717
13.0	33.710	33.704	33.719	33.717	33.717	33.719	33.719	33.718	33.716	33.722	33.718	33.721	33.722	33.717	33.723	33.720
13.5	33.701	33.689	33.718	33.713	33.715	33.717	33.718	33.717	33.711	33.722	33.718	33.719	33.719	33.712	33.720	33.720
14.0	33.697	33.732	33.686	33.720	33.715	33.718	33.717	33.719	33.718	33.722	33.719	33.720	33.715	33.718	33.721	33.721
14.5	33.721	33.713	33.695	33.718	33.723	33.732	33.712	33.719	33.713	33.721	33.720	33.719	33.723	33.712	33.721	33.719
15.0	33.733	33.729	33.705	33.717	33.733	33.717	33.717	33.719	33.693	33.720	33.719	33.718	33.719	33.718	33.720	33.720
15.5	33.731	33.734	33.652	33.701	33.719	33.719	33.713	33.724	33.576	33.718			33.724	33.720	33.720	33.721
16.0	33.736		33.661	33.718	33.726	33.719	33.716	33.719	33.562	33.720			33.718	33.719		
16.5			33.708	33.720	33.726	33.726	33.727	33.729	33.661				33.724	33.720		
17.0							33.722									
17.5							33.732									

¹ Values enclosed in boxes were significantly lower than the mean of other salinity measurements at the same depth or at the same distance above the seafloor.

Table B-3. Seawater Density¹ on 9 October 2007

Depth (m)	Density (sigma-t)															
	1	2	3	4	5	6	7	8	9	10	11	12	13	14	15	16
0.5	25.382	25.387	25.382	25.384	25.402		25.400	25.404						25.415		25.427
1.0	25.387	25.391	25.386	25.382	25.403	25.409	25.400	25.404	25.403	25.414	25.423	25.430	25.399	25.415	25.415	25.427
1.5	25.411	25.395	25.392	25.383	25.403	25.411	25.399	25.404	25.404	25.413	25.424	25.430	25.400	25.414	25.417	25.428
2.0	25.421	25.405	25.393	25.391	25.403	25.412	25.400	25.403	25.407	25.413	25.424	25.431	25.402	25.416	25.417	25.427
2.5	25.433	25.411	25.406	25.392	25.403	25.413	25.401	25.404	25.406	25.414	25.425	25.431	25.402	25.416	25.417	25.427
3.0	25.430	25.474	25.419	25.398	25.403	25.415	25.405	25.404	25.410	25.413	25.425	25.431	25.403	25.414	25.418	25.428
3.5	25.446	25.476	25.419	25.395	25.403	25.415	25.403	25.406	25.414	25.415	25.425	25.431	25.404	25.419	25.417	25.431
4.0	25.440	25.482	25.421	25.399	25.404	25.432	25.412	25.427	25.417	25.418	25.425	25.432	25.404	25.419	25.417	25.430
4.5	25.462	25.489	25.422	25.407	25.404	25.431	25.416	25.441	25.413	25.418	25.428	25.432	25.405	25.426	25.418	25.439
5.0	25.465	25.481	25.422	25.419	25.405	25.462	25.420	25.441	25.414	25.420	25.427	25.429	25.401	25.424	25.421	25.446
5.5	25.461	25.478	25.423	25.425	25.434	25.479	25.418	25.437	25.414	25.421	25.430	25.467	25.412	25.438	25.426	25.457
6.0	25.469	25.484	25.423	25.450	25.435	25.473	25.444	25.454	25.420	25.425	25.430	25.456	25.417	25.440	25.427	25.469
6.5	25.484	25.503	25.444	25.453	25.444	25.479	25.477	25.467	25.436	25.455	25.434	25.475	25.426	25.439	25.428	25.479
7.0	25.478	25.497	25.442	25.471	25.469	25.487	25.474	25.466	25.434	25.450	25.445	25.485	25.462	25.435	25.431	25.486
7.5	25.484	25.492	25.446	25.493	25.482	25.492	25.491	25.479	25.441	25.455	25.474	25.485	25.471	25.466	25.424	25.491
8.0	25.482	25.496	25.490	25.497	25.486	25.487	25.492	25.480	25.473	25.478	25.473	25.486	25.481	25.487	25.430	25.496
8.5	25.482	25.502	25.476	25.496	25.489	25.489	25.491	25.485	25.487	25.478	25.476	25.484	25.476	25.487	25.485	25.497
9.0	25.487	25.499	25.491	25.495	25.491	25.492	25.493	25.490	25.488	25.487	25.483	25.484	25.489	25.491	25.472	25.504
9.5	25.493	25.495	25.490	25.495	25.489	25.492	25.496	25.490	25.489	25.490	25.484	25.484	25.488	25.497	25.481	25.505
10.0	25.498	25.493	25.489	25.494	25.490	25.492	25.494	25.490	25.490	25.488	25.489	25.483	25.493	25.500	25.478	25.506
10.5	25.498	25.498	25.491	25.494	25.490	25.491	25.495	25.490	25.490	25.492	25.490	25.483	25.494	25.502	25.494	25.505
11.0	25.497	25.492	25.494	25.493	25.493	25.493	25.492	25.498	25.495	25.494	25.495	25.486	25.494	25.510	25.508	25.506
11.5	25.497	25.498	25.496	25.494	25.494	25.504	25.507	25.506	25.499	25.494	25.515	25.497	25.495	25.516	25.512	25.514
12.0	25.496	25.499	25.485	25.495	25.496	25.504	25.511	25.508	25.501	25.504	25.506	25.493	25.499	25.521	25.516	25.520
12.5	25.502	25.499	25.496	25.496	25.497	25.503	25.519	25.508	25.503	25.508	25.513	25.516	25.501	25.521	25.520	25.515
13.0	25.507	25.504	25.499	25.498	25.498	25.501	25.521	25.512	25.505	25.521	25.511	25.511	25.507	25.523	25.523	25.519
13.5	25.502	25.492	25.498	25.498	25.497	25.501	25.520	25.516	25.507	25.523	25.512	25.509	25.508	25.521	25.520	25.521
14.0	25.506	25.551	25.475	25.513	25.500	25.505	25.520	25.521	25.518	25.524	25.512	25.509	25.508	25.533	25.521	25.523
14.5	25.546	25.538	25.483	25.512	25.511	25.523	25.518	25.524	25.516	25.523	25.513	25.508	25.525	25.532	25.521	25.522
15.0	25.565	25.561	25.492	25.516	25.537	25.512	25.527	25.524	25.502	25.521	25.511	25.508	25.522	25.540	25.520	25.524
15.5	25.571	25.569	25.457	25.508	25.536	25.524	25.528	25.533	25.533	25.520			25.534	25.543	25.520	25.525
16.0	25.576		25.471	25.524	25.543	25.530	25.536	25.534	25.540	25.522			25.531	25.542		
16.5			25.536	25.537	25.544	25.534	25.551	25.548	25.484				25.542	25.543		
17.0							25.549		25.528					25.544		
17.5							25.565									

¹ Values enclosed in boxes were significantly lower than the mean of other density measurements at the same distance above the seafloor.

Table B-4. Detrended¹ Dissolved Oxygen on 9 October 2007

Depth (m)	Dissolved Oxygen (mg/L)															
	1	2	3	4	5	6	7	8	9	10	11	12	13	14	15	16
0.5	6.34	6.54	6.49	6.58	6.58		6.67	6.85						6.90		6.79
1.0	6.44	6.55	6.52	6.52	6.58	6.45	6.67	6.85	6.83	6.87	6.80	6.83	6.31	6.90	6.88	6.79
1.5	6.54	6.63	6.55	6.56	6.61	6.54	6.70	6.87	6.84	6.88	6.81	6.83	6.35	6.91	6.88	6.80
2.0	6.62	6.65	6.58	6.59	6.62	6.56	6.73	6.86	6.83	6.87	6.81	6.84	6.41	6.92	6.88	6.81
2.5	6.64	6.67	6.60	6.62	6.64	6.60	6.73	6.87	6.83	6.87	6.81	6.83	6.46	6.92	6.89	6.82
3.0	6.67	6.62	6.63	6.64	6.66	6.64	6.71	6.88	6.84	6.87	6.82	6.83	6.49	6.92	6.89	6.81
3.5	6.68	6.55	6.62	6.67	6.69	6.64	6.71	6.86	6.85	6.86	6.80	6.82	6.49	6.91	6.88	6.81
4.0	6.69	6.56	6.63	6.70	6.70	6.62	6.70	6.81	6.86	6.85	6.81	6.83	6.52	6.90	6.88	6.79
4.5	6.68	6.52	6.64	6.71	6.73	6.58	6.67	6.78	6.86	6.85	6.80	6.83	6.54	6.90	6.88	6.75
5.0	6.67	6.51	6.66	6.67	6.74	6.55	6.65	6.77	6.86	6.85	6.79	6.79	6.56	6.88	6.87	6.74
5.5	6.70	6.51	6.66	6.68	6.72	6.54	6.65	6.73	6.85	6.83	6.81	6.76	6.56	6.86	6.87	6.67
6.0	6.67	6.50	6.68	6.62	6.73	6.50	6.62	6.70	6.83	6.82	6.77	6.69	6.56	6.84	6.87	6.61
6.5	6.67	6.44	6.65	6.58	6.68	6.46	6.58	6.69	6.81	6.74	6.73	6.62	6.57	6.81	6.86	6.53
7.0	6.64	6.46	6.69	6.62	6.65	6.45	6.61	6.64	6.79	6.70	6.70	6.56	6.56	6.82	6.83	6.45
7.5	6.66	6.47	6.68	6.59	6.64	6.41	6.61	6.59	6.73	6.62	6.61	6.53	6.48	6.75	6.80	6.38
8.0	6.66	6.45	6.65	6.56	6.67	6.37	6.58	6.54	6.63	6.58	6.56	6.50	6.47	6.66	6.77	6.34
8.5	6.66	6.43	6.62	6.54	6.65	6.36	6.56	6.50	6.53	6.53	6.53	6.48	6.44	6.59	6.66	6.32
9.0	6.64	6.42	6.69	6.57	6.61	6.36	6.52	6.47	6.50	6.50	6.51	6.46	6.40	6.51	6.58	6.29
9.5	6.65	6.41	6.72	6.55	6.60	6.37	6.44	6.44	6.46	6.48	6.47	6.45	6.37	6.47	6.53	6.26
10.0	6.64	6.41	6.75	6.54	6.59	6.36	6.41	6.43	6.44	6.46	6.44	6.43	6.32	6.41	6.46	6.22
10.5	6.64	6.44	6.75	6.55	6.57	6.35	6.37	6.42	6.43	6.44	6.40	6.43	6.31	6.36	6.40	6.23
11.0	6.62	6.45	6.70	6.55	6.57	6.35	6.33	6.39	6.41	6.38	6.34	6.38	6.30	6.29	6.35	6.20
11.5	6.63	6.45	6.66	6.54	6.57	6.33	6.30	6.34	6.39	6.33	6.32	6.35	6.30	6.26	6.34	6.19
12.0	6.64	6.42	6.63	6.54	6.57	6.31	6.27	6.32	6.39	6.32	6.29	6.31	6.28	6.24	6.29	6.17
12.5	6.64	6.44	6.63	6.54	6.56	6.29	6.23	6.31	6.39	6.27	6.25	6.26	6.29	6.23	6.25	6.16
13.0	6.64	6.44	6.62	6.54	6.54	6.28	6.24	6.30	6.37	6.25	6.23	6.25	6.26	6.22	6.23	6.15
13.5	6.61	6.41	6.62	6.51	6.52	6.27	6.22	6.26	6.33	6.20	6.22	6.22	6.26	6.21	6.21	6.14
14.0	6.58	6.34	6.60	6.45	6.48	6.25	6.21	6.24	6.29	6.18	6.20	6.21	6.24	6.20	6.19	6.12
14.5	6.48	6.29	6.60	6.41	6.42	6.23	6.20	6.21	6.25	6.17	6.19	6.20	6.22	6.17	6.18	6.10
15.0	6.43	6.25	6.60	6.33	6.32	6.22	6.20	6.19	6.23	6.15	6.19	6.20	6.19	6.12	6.17	6.09
15.5	6.37	6.24	6.54	6.29	6.22	6.16	6.16	6.16	6.17	6.16			6.13	6.11	6.17	6.09
16.0	6.37		6.47	6.28	6.19	6.13	6.13	6.12	6.10	6.16			6.09	6.09		
16.5			6.47	6.25	6.19	6.13	6.09	6.12	6.09				6.09	6.06		
17.0							6.05		6.09					6.06		
17.5							6.05									

¹ Measured DO concentrations were corrected for temporal drift to account for ongoing equilibration of the sensor.

Table B-5. Light Transmittance¹ across a 0.25-m path on 9 October 2007

Depth (m)	Light Transmittance (%)															
	1	2	3	4	5	6	7	8	9	10	11	12	13	14	15	16
0.5	76.61	76.39	76.56	76.48	75.93		75.90	75.79						75.33		76.12
1.0	76.62	76.42	76.47	76.40	75.92	76.05	75.83	75.68	75.64	75.66	75.70	45.99	75.88	75.46	75.35	76.17
1.5	76.41	76.32	76.42	76.43	76.03	76.12	75.73	75.73	75.63	75.58	75.77	58.36	75.90	75.60	75.43	76.01
2.0	76.36	76.26	76.33	76.28	76.01	76.15	75.81	75.72	75.65	75.63	75.75	73.54	75.98	75.58	75.33	76.09
2.5	76.29	76.23	76.21	76.19	76.10	76.16	75.84	75.85	75.57	75.76	75.87	62.57	75.90	75.67	75.43	76.03
3.0	76.41	76.86	76.55	76.19	76.08	76.01	76.03	75.99	75.62	75.77	75.97	53.10	76.01	75.84	75.61	75.97
3.5	76.51	77.15	77.09	76.17	76.09	76.15	76.03	75.94	75.95	75.80	76.11	51.89	75.98	75.81	75.59	76.19
4.0	76.62	77.11	76.91	76.16	76.06	76.53	76.44	76.75	76.02	75.92	76.19	57.57	76.11	76.16	75.73	76.69
4.5	76.64	77.24	76.91	75.99	76.12	77.45	77.11	77.07	75.86	76.22	76.25	63.12	76.06	76.24	75.69	76.86
5.0	76.66	77.32	76.82	76.04	76.17	78.20	77.27	77.08	75.98	76.15	76.33	40.75	76.17	76.58	75.54	77.95
5.5	76.41	77.87	76.92	76.57	76.34	78.28	77.30	77.21	76.13	76.17	76.38	50.72	76.39	77.28	75.66	78.57
6.0	76.68	77.21	76.99	76.86	76.54	78.13	77.54	78.17	76.50	76.47	76.63	45.20	76.91	78.06	75.71	78.47
6.5	76.60	76.85	76.91	77.22	76.80	78.23	77.86	78.79	77.01	76.66	77.18	39.08	76.96	78.64	75.71	77.94
7.0	76.63	76.78	77.25	78.09	77.23	78.31	78.65	78.90	77.06	77.29	77.66	44.92	77.44	78.76	77.03	77.63
7.5	76.95	77.12	77.76	78.96	77.98	78.18	79.27	78.38	77.39	77.87	78.26	66.51	78.49	78.87	77.68	77.24
8.0	76.87	77.08	77.86	78.95	78.54	78.10	79.37	78.19	78.20	78.28	78.08	76.46	78.43	78.43	78.03	77.19
8.5	76.74	76.77	78.47	78.76	78.59	77.93	79.26	78.21	78.19	78.23	78.08	65.63	78.50	77.86	78.43	77.05
9.0	76.73	76.78	79.12	78.74	78.61	78.02	79.09	78.16	78.19	77.94	78.20	78.64	78.39	77.54	78.15	76.97
9.5	76.76	76.69	79.44	78.70	78.79	78.06	78.88	78.20	78.24	77.92	78.22	77.89	78.40	77.32	77.87	77.05
10.0	76.68	76.61	79.36	78.67	79.02	78.03	78.67	78.27	78.20	78.03	78.00	77.90	78.25	77.35	77.79	76.92
10.5	76.83	76.71	79.05	78.50	78.96	78.19	78.62	78.26	78.19	78.00	77.87	78.14	78.03	77.19	77.39	77.06
11.0	76.70	76.83	78.68	78.41	78.97	78.44	78.36	78.39	78.26	77.78	77.77	78.02	78.03	77.14	77.61	76.96
11.5	76.64	76.88	78.39	78.49	79.26	78.03	77.95	78.42	78.56	77.57	77.83	77.94	78.07	77.53	77.80	77.26
12.0	76.74	76.77	78.34	78.53	79.05	77.63	77.68	78.29	78.76	77.97	77.49	77.94	78.12	77.72	77.81	77.72
12.5	76.91	76.72	78.26	78.55	79.00	77.56	77.56	78.27	78.80	78.36	77.24	77.38	78.07	78.01	77.53	77.45
13.0	76.83	76.79	78.32	78.51	78.91	77.51	77.60	78.11	78.88	77.60	76.93	77.16	77.90	78.20	76.93	77.43
13.5	76.80	76.79	78.23	78.65	78.82	77.49	77.42	78.01	78.88	77.06	76.73	77.15	78.04	78.36	76.70	77.34
14.0	76.59	76.68	78.44	78.23	78.54	77.35	77.38	77.82	78.58	76.65	76.68	76.90	78.06	78.71	76.61	77.14
14.5	76.28	76.32	78.42	77.87	78.23	77.25	77.50	77.60	78.35	76.58	76.80	76.78	78.01	77.92	76.41	77.07
15.0	75.95	76.04	78.27	77.45	77.31	77.15	78.01	77.22	77.64	76.86	76.79	76.36	77.70	77.34	76.37	76.87
15.5	75.90	75.94	77.45	76.82	76.17	76.83	78.12	77.38	74.93	76.78			77.47	77.36	76.38	76.31
16.0	75.85		77.31	76.69	75.88	76.16	78.01	76.82	74.88	76.71			76.93	77.32		
16.5			75.80	76.23	75.01	75.95	77.43	76.42	75.31				76.48	77.07		
17.0							76.77		75.94					77.01		
17.5							76.59									

¹ Values enclosed in the boxes were significantly lower than the mean of other transmissivity measurements at the same distance above the seafloor. The Station 12 anomaly was caused by blockage of the light transmission path by a piece of kelp that temporarily became entangled on the CTD (see text). The significance of the Station 9 anomaly arose only after exclusion of the erroneous Station 12 data.

Table B-6. Detrended¹ pH² on 9 October 2007

Depth (m)	Hydrogen Ion Concentration (pH)															
	1	2	3	4	5	6	7	8	9	10	11	12	13	14	15	16
0.5	8.241	8.214	8.211	8.207	8.207		8.226	8.222						8.224		8.231
1.0	8.240	8.214	8.211	8.214	8.212	8.226	8.224	8.222	8.217	8.227	8.230	8.233	8.221	8.226	8.230	8.231
1.5	8.237	8.214	8.211	8.214	8.213	8.226	8.225	8.222	8.217	8.227	8.230	8.236	8.222	8.225	8.230	8.234
2.0	8.239	8.214	8.212	8.212	8.213	8.226	8.225	8.222	8.217	8.227	8.230	8.236	8.222	8.225	8.230	8.236
2.5	8.237	8.214	8.213	8.213	8.213	8.226	8.225	8.222	8.217	8.227	8.230	8.236	8.222	8.225	8.230	8.236
3.0	8.237	8.214	8.217	8.214	8.213	8.226	8.225	8.222	8.217	8.227	8.230	8.236	8.222	8.225	8.230	8.236
3.5	8.237	8.215	8.220	8.214	8.213	8.226	8.225	8.222	8.217	8.227	8.230	8.234	8.222	8.225	8.230	8.236
4.0	8.233	8.215	8.220	8.214	8.213	8.226	8.225	8.222	8.217	8.227	8.230	8.232	8.222	8.225	8.230	8.236
4.5	8.233	8.213	8.219	8.214	8.213	8.226	8.225	8.223	8.220	8.227	8.230	8.234	8.222	8.225	8.230	8.234
5.0	8.233	8.211	8.222	8.215	8.213	8.227	8.228	8.223	8.221	8.227	8.230	8.234	8.222	8.228	8.230	8.233
5.5	8.233	8.211	8.222	8.219	8.214	8.229	8.228	8.224	8.221	8.227	8.231	8.237	8.222	8.226	8.230	8.232
6.0	8.231	8.211	8.222	8.220	8.214	8.227	8.230	8.228	8.222	8.227	8.232	8.234	8.223	8.229	8.230	8.232
6.5	8.230	8.211	8.222	8.220	8.218	8.227	8.231	8.228	8.222	8.227	8.234	8.229	8.226	8.231	8.230	8.229
7.0	8.228	8.209	8.222	8.221	8.219	8.223	8.231	8.228	8.222	8.227	8.232	8.225	8.227	8.231	8.230	8.228
7.5	8.228	8.205	8.222	8.224	8.219	8.222	8.233	8.228	8.223	8.228	8.230	8.223	8.228	8.235	8.231	8.222
8.0	8.228	8.206	8.222	8.226	8.220	8.218	8.236	8.228	8.223	8.225	8.227	8.223	8.228	8.231	8.231	8.217
8.5	8.227	8.207	8.219	8.226	8.225	8.216	8.236	8.225	8.223	8.223	8.223	8.218	8.228	8.228	8.230	8.215
9.0	8.224	8.202	8.225	8.226	8.225	8.213	8.236	8.220	8.219	8.223	8.221	8.218	8.225	8.223	8.226	8.210
9.5	8.224	8.202	8.229	8.226	8.225	8.215	8.232	8.217	8.217	8.223	8.221	8.218	8.224	8.218	8.223	8.206
10.0	8.224	8.202	8.232	8.226	8.225	8.218	8.229	8.214	8.214	8.218	8.220	8.215	8.219	8.212	8.215	8.204
10.5	8.224	8.202	8.233	8.223	8.225	8.216	8.227	8.214	8.214	8.219	8.217	8.216	8.219	8.208	8.216	8.204
11.0	8.222	8.202	8.230	8.221	8.225	8.217	8.224	8.214	8.214	8.219	8.215	8.215	8.218	8.206	8.213	8.204
11.5	8.219	8.202	8.228	8.221	8.225	8.218	8.219	8.215	8.214	8.218	8.214	8.214	8.217	8.204	8.210	8.204
12.0	8.219	8.202	8.224	8.221	8.225	8.215	8.217	8.215	8.214	8.216	8.209	8.210	8.217	8.204	8.208	8.205
12.5	8.219	8.203	8.223	8.221	8.223	8.213	8.213	8.213	8.214	8.214	8.207	8.209	8.216	8.204	8.205	8.199
13.0	8.219	8.207	8.223	8.221	8.222	8.210	8.212	8.210	8.214	8.214	8.207	8.206	8.215	8.204	8.204	8.200
13.5	8.219	8.211	8.223	8.221	8.222	8.208	8.208	8.210	8.214	8.210	8.204	8.204	8.215	8.204	8.204	8.200
14.0	8.217	8.212	8.223	8.221	8.220	8.208	8.208	8.210	8.215	8.208	8.203	8.204	8.215	8.204	8.199	8.200
14.5	8.212	8.207	8.223	8.218	8.219	8.209	8.208	8.209	8.215	8.205	8.203	8.203	8.215	8.206	8.199	8.200
15.0	8.208	8.203	8.223	8.217	8.216	8.209	8.209	8.204	8.213	8.203	8.202	8.205	8.213	8.202	8.199	8.200
15.5	8.205	8.199	8.221	8.211	8.211	8.204	8.209	8.205	8.210	8.200			8.210	8.199	8.199	8.198
16.0	8.199		8.216	8.205	8.204	8.204	8.209	8.206	8.199	8.200			8.210	8.199		
16.5			8.212	8.202	8.200	8.200	8.209	8.204	8.199				8.208	8.197		
17.0							8.205		8.195					8.194		
17.5							8.204									

¹ Measured pH levels were corrected for temporal drift to account for ongoing equilibration of the pH sensor.

² The value enclosed in the box was significantly lower than the mean of other pH measurements at the same depth or at the same distance above the seafloor.

Table B-7. Uncorrected pH¹ on 9 October 2007

Depth (m)	Hydrogen Ion Concentration (pH)															
	1	2	3	4	5	6	7	8	9	10	11	12	13	14	15	16
0.5	8.173	8.168	8.172	8.170	8.171		8.207	8.206						8.224		8.230
1.0	8.172	8.168	8.172	8.177	8.176	8.197	8.205	8.206	8.206	8.221	8.226	8.232	8.200	8.226	8.230	8.230
1.5	8.169	8.168	8.172	8.177	8.177	8.197	8.206	8.206	8.206	8.221	8.226	8.235	8.201	8.225	8.230	8.233
2.0	8.171	8.168	8.173	8.175	8.177	8.197	8.206	8.206	8.206	8.221	8.226	8.235	8.201	8.225	8.230	8.235
2.5	8.169	8.168	8.174	8.176	8.177	8.197	8.206	8.206	8.206	8.221	8.226	8.235	8.201	8.225	8.230	8.235
3.0	8.169	8.168	8.178	8.177	8.177	8.197	8.206	8.206	8.206	8.221	8.226	8.235	8.201	8.225	8.230	8.235
3.5	8.169	8.169	8.181	8.177	8.177	8.197	8.206	8.206	8.206	8.221	8.226	8.233	8.201	8.225	8.230	8.235
4.0	8.165	8.169	8.181	8.177	8.177	8.197	8.206	8.206	8.206	8.221	8.226	8.231	8.201	8.225	8.230	8.235
4.5	8.165	8.167	8.180	8.177	8.177	8.197	8.206	8.207	8.209	8.221	8.226	8.233	8.201	8.225	8.230	8.233
5.0	8.165	8.165	8.183	8.178	8.177	8.198	8.209	8.207	8.210	8.221	8.226	8.233	8.201	8.228	8.230	8.232
5.5	8.165	8.165	8.183	8.182	8.178	8.200	8.209	8.208	8.210	8.221	8.227	8.236	8.201	8.226	8.230	8.231
6.0	8.163	8.165	8.183	8.183	8.178	8.198	8.211	8.212	8.211	8.221	8.228	8.233	8.202	8.229	8.230	8.231
6.5	8.162	8.165	8.183	8.183	8.182	8.198	8.212	8.212	8.211	8.221	8.230	8.228	8.205	8.231	8.230	8.228
7.0	8.160	8.163	8.183	8.184	8.183	8.194	8.212	8.212	8.211	8.221	8.228	8.224	8.206	8.231	8.230	8.227
7.5	8.160	8.159	8.183	8.187	8.183	8.193	8.214	8.212	8.212	8.222	8.226	8.222	8.207	8.235	8.231	8.221
8.0	8.160	8.160	8.183	8.189	8.184	8.189	8.217	8.212	8.212	8.219	8.223	8.222	8.207	8.231	8.231	8.216
8.5	8.159	8.161	8.180	8.189	8.189	8.187	8.217	8.209	8.212	8.217	8.219	8.217	8.207	8.228	8.230	8.214
9.0	8.156	8.156	8.186	8.189	8.189	8.184	8.217	8.204	8.208	8.217	8.217	8.217	8.204	8.223	8.226	8.209
9.5	8.156	8.156	8.190	8.189	8.189	8.186	8.213	8.201	8.206	8.217	8.217	8.217	8.203	8.218	8.223	8.205
10.0	8.156	8.156	8.193	8.189	8.189	8.189	8.210	8.198	8.203	8.212	8.216	8.214	8.198	8.212	8.215	8.203
10.5	8.156	8.156	8.194	8.186	8.189	8.187	8.208	8.198	8.203	8.213	8.213	8.215	8.198	8.208	8.216	8.203
11.0	8.154	8.156	8.191	8.184	8.189	8.188	8.205	8.198	8.203	8.213	8.211	8.214	8.197	8.206	8.213	8.203
11.5	8.151	8.156	8.189	8.184	8.189	8.189	8.200	8.199	8.203	8.212	8.210	8.213	8.196	8.204	8.210	8.203
12.0	8.151	8.156	8.185	8.184	8.189	8.186	8.198	8.199	8.203	8.210	8.205	8.209	8.196	8.204	8.208	8.204
12.5	8.151	8.157	8.184	8.184	8.187	8.184	8.194	8.197	8.203	8.208	8.203	8.208	8.195	8.204	8.205	8.198
13.0	8.151	8.161	8.184	8.184	8.186	8.181	8.193	8.194	8.203	8.208	8.203	8.205	8.194	8.204	8.204	8.199
13.5	8.151	8.165	8.184	8.184	8.186	8.179	8.189	8.194	8.203	8.204	8.200	8.203	8.194	8.204	8.204	8.199
14.0	8.149	8.166	8.184	8.184	8.184	8.179	8.189	8.194	8.204	8.202	8.199	8.203	8.194	8.204	8.199	8.199
14.5	8.144	8.161	8.184	8.181	8.183	8.180	8.189	8.193	8.204	8.199	8.199	8.202	8.194	8.206	8.199	8.199
15.0	8.140	8.157	8.184	8.180	8.180	8.180	8.190	8.188	8.202	8.197	8.198	8.204	8.192	8.202	8.199	8.199
15.5	8.137	8.153	8.182	8.174	8.175	8.175	8.190	8.189	8.199	8.194			8.189	8.199	8.199	8.197
16.0	8.131		8.177	8.168	8.168	8.175	8.190	8.190	8.188	8.194			8.189	8.199		
16.5			8.173	8.165	8.164	8.171	8.190	8.188	8.188				8.187	8.197		
17.0							8.186		8.184					8.194		
17.5							8.185									

¹ Values enclosed in boxes were significantly lower than the mean of other pH measurements at the same depth or at the same distance above the seafloor.

Table B-8. Uncorrected Dissolved Oxygen¹ on 9 October 2007

Depth (m)	Dissolved Oxygen (mg/L)															
	1	2	3	4	5	6	7	8	9	10	11	12	13	14	15	16
0.5	5.74	6.15	6.22	6.42	6.49		6.67	6.85						6.90		6.79
1.0	5.84	6.16	6.25	6.37	6.49	6.41	6.67	6.85	6.83	6.87	6.80	6.83	6.30	6.90	6.88	6.79
1.5	5.95	6.24	6.28	6.40	6.52	6.51	6.70	6.87	6.84	6.88	6.81	6.83	6.35	6.91	6.88	6.80
2.0	6.03	6.26	6.31	6.44	6.53	6.53	6.73	6.86	6.83	6.87	6.81	6.84	6.41	6.92	6.88	6.81
2.5	6.05	6.28	6.33	6.46	6.55	6.57	6.73	6.87	6.83	6.87	6.81	6.83	6.45	6.92	6.89	6.82
3.0	6.08	6.24	6.36	6.48	6.57	6.61	6.71	6.88	6.84	6.87	6.82	6.83	6.48	6.92	6.89	6.81
3.5	6.09	6.16	6.35	6.52	6.60	6.61	6.71	6.86	6.85	6.86	6.80	6.82	6.48	6.91	6.88	6.81
4.0	6.09	6.17	6.36	6.55	6.61	6.59	6.70	6.81	6.86	6.85	6.81	6.83	6.51	6.90	6.88	6.79
4.5	6.09	6.13	6.37	6.55	6.64	6.55	6.67	6.78	6.86	6.85	6.80	6.83	6.53	6.90	6.88	6.75
5.0	6.07	6.12	6.39	6.51	6.65	6.52	6.65	6.77	6.86	6.85	6.79	6.79	6.55	6.88	6.87	6.74
5.5	6.11	6.13	6.39	6.53	6.63	6.50	6.65	6.73	6.85	6.83	6.81	6.76	6.55	6.86	6.87	6.67
6.0	6.07	6.11	6.41	6.47	6.64	6.46	6.62	6.70	6.83	6.82	6.77	6.69	6.56	6.84	6.87	6.61
6.5	6.07	6.05	6.39	6.43	6.59	6.43	6.58	6.69	6.81	6.74	6.73	6.62	6.56	6.81	6.86	6.53
7.0	6.04	6.07	6.42	6.46	6.56	6.42	6.61	6.64	6.79	6.70	6.70	6.56	6.55	6.82	6.83	6.45
7.5	6.07	6.08	6.41	6.44	6.55	6.38	6.61	6.59	6.73	6.62	6.61	6.53	6.48	6.75	6.80	6.38
8.0	6.06	6.06	6.38	6.40	6.58	6.34	6.58	6.54	6.63	6.58	6.56	6.50	6.47	6.66	6.77	6.34
8.5	6.06	6.04	6.35	6.39	6.56	6.33	6.56	6.50	6.53	6.53	6.53	6.48	6.44	6.59	6.66	6.32
9.0	6.04	6.03	6.42	6.41	6.52	6.33	6.52	6.47	6.50	6.50	6.51	6.46	6.40	6.51	6.58	6.29
9.5	6.05	6.02	6.45	6.40	6.51	6.33	6.44	6.44	6.46	6.48	6.47	6.45	6.36	6.47	6.53	6.26
10.0	6.04	6.02	6.48	6.39	6.50	6.33	6.41	6.43	6.44	6.46	6.44	6.43	6.31	6.41	6.46	6.22
10.5	6.04	6.06	6.48	6.39	6.48	6.32	6.37	6.42	6.43	6.44	6.40	6.43	6.30	6.36	6.40	6.23
11.0	6.03	6.06	6.43	6.39	6.48	6.32	6.33	6.39	6.41	6.38	6.34	6.38	6.29	6.29	6.35	6.20
11.5	6.03	6.06	6.39	6.39	6.48	6.29	6.30	6.34	6.39	6.33	6.32	6.35	6.29	6.26	6.34	6.19
12.0	6.04	6.04	6.36	6.39	6.48	6.28	6.27	6.32	6.39	6.32	6.29	6.31	6.28	6.24	6.29	6.17
12.5	6.05	6.05	6.36	6.39	6.47	6.26	6.23	6.31	6.39	6.27	6.25	6.26	6.28	6.23	6.25	6.16
13.0	6.04	6.05	6.35	6.38	6.45	6.25	6.24	6.30	6.37	6.25	6.23	6.25	6.26	6.22	6.23	6.15
13.5	6.02	6.02	6.35	6.35	6.43	6.24	6.22	6.26	6.33	6.20	6.22	6.22	6.26	6.21	6.21	6.14
14.0	5.98	5.95	6.33	6.30	6.39	6.22	6.21	6.24	6.29	6.18	6.20	6.21	6.24	6.20	6.19	6.12
14.5	5.88	5.91	6.33	6.25	6.33	6.20	6.20	6.21	6.25	6.17	6.19	6.20	6.21	6.17	6.18	6.10
15.0	5.84	5.86	6.33	6.18	6.23	6.19	6.20	6.19	6.23	6.15	6.19	6.20	6.18	6.12	6.17	6.09
15.5	5.77	5.85	6.27	6.14	6.13	6.12	6.16	6.16	6.17	6.16			6.13	6.11	6.17	6.09
16.0	5.77		6.20	6.12	6.10	6.09	6.13	6.12	6.10	6.16			6.08	6.09		
16.5			6.20	6.10	6.10	6.09	6.09	6.12	6.09				6.08	6.06		
17.0							6.05		6.09					6.06		
17.5							6.05									

¹ Values enclosed in boxes were significantly lower than the mean of other dissolved oxygen measurements at the same depth level.

Table B-9. Ancillary Observations on 9 October 2007 during the Receiving-Water Survey

Station	Location		Diffuser Distance (m)	Time (PDT)	Temperature (°C)		Cloud Cover (%)	Wind Avg (kt)	Wind Max (kt)	Wind Dir (from) (°T)	Swell Ht/Dir (ft/°T)	Secchi Depth (m)
	Latitude	Longitude			Air	Water						
1	35°23.2285' N	120°52.5064' W	113.4	8:00:26	—*	—	90	—	—	SE	1-2/W	—
2	35°23.2297' N	120°52.5117' W	44.6	8:01:28	10.8	11.1	85	3.3	5.2	SE	1-2/W	7.0
3	35°23.2075' N	120°52.5109' W	15.7	8:05:09	10.9	—	80	3.7	6.6	SE	1-2/W	8.0
4	35°23.1939' N	120°52.5080' W	9.7	8:12:34	10.3	—	75	1.6	2.5	SE	1-2/W	7.0
5	35°23.1630' N	120°52.5035' W	42.5	8:16:06	10.0	—	75	2.2	4.6	SE	1-2/W	7.0
6	35°23.1452' N	120°52.5073' W	70.7	8:22:47	10.3	11.4	75	2.1	3.7	SE	1-2/W	7.5
7	35°23.1994' N	120°52.5732' W	77.9	8:32:45	10.3	11.4	75	1.4	2.2	SE	1-2/W	6.5
8	35°23.2014' N	120°52.5362' W	34.2	8:38:18	10.5	11.7	75	1.4	2.6	SE	1-2/W	6.5
9	35°23.2016' N	120°52.5144' W	24.6	8:42:23	10.2	11.7	75	2.1	3.8	SE	1-2/W	6.0
10	35°23.1989' N	120°52.4861' W	16.8	8:47:29	10.5	11.7	75	2.7	4.4	SE	1-2/W	7.0
11	35°23.2001' N	120°52.4603' W	43.0	8:52:18	10.4	11.7	75	1.9	3.5	SE	1-2/W	6.5
12	35°23.1975' N	120°52.4379' W	99.3	8:57:38	11.4	11.9	75	1.0	1.9	SE	1-2/W	6.5
13	35°23.1781' N	120°52.5282' W	50.5	8:28:38	10.3	11.9	75	1.2	1.9	SE	1-2/W	7.0
14	35°23.2219' N	120°52.5324' W	46.5	9:10:15	10.8	12.2	75	1.3	1.8	SE	1-2/W	6.5
15	35°23.2236' N	120°52.4722' W	72.1	9:06:05	11.7	11.7	75	1.0	2.1	SE	1-2/W	6.5
16	35°23.1738' N	120°52.4742' W	38.7	9:01:53	10.6	11.7	75	1.6	3.4	SE	1-2/W	6.5

There was no visual expression of the effluent plume at the sea surface. Neither odors nor debris of sewage origin were observed at any time during the survey.

* Ancillary wind and temperature readings at Station 1 were not recorded due to a battery failure in the Kestrel. A new battery was installed prior to sampling at the other stations.

Tidal Conditions (Pacific Daylight Time)

Low Tide: 03:40 0.53 ft

High Tide: 09:54 5.15 ft

Low Tide: 16:05 0.72 ft

High Tide: 22:05 4.71 ft